

ADA013104

(18) ESD | (19) TR-75-180 |

MASSACHUSETTS INSTITUTE OF TECHNOLOGY
LINCOLN LABORATORY

⑥ OPTIMIZATION OF A COMMUNICATION SATELLITE
MULTIPLE-BEAM ANTENNA.

⑩ Andre R. DION
Group 01

⑮ F19628-73-C-0002 |

⑨ TECHNICAL NOTE

⑪ 27 MAY 1975

⑫ 62p.

⑭ TN-1975-39

Approved for public release; distribution unlimited.

REC
JUN 20 1975
RECEIVED

LEXINGTON

MASSACHUSETTS

1473

207 650

mt

ABSTRACT

The dimensions of a multiple-beam antenna designed to optimize some desirable characteristics of a synchronous communication satellite antenna are derived. The multiple-beam antenna is an X-band waveguide lens with a cluster of feeds in its focal plane. Two antenna systems are considered: 1) an antenna system radiating pencil beams for area coverage, and 2) an antenna system radiating an earth-coverage beam with nulls in prescribed directions. The characteristics of the optimum configurations are studied over a band of frequency and for practical values of feed excitation errors.

Optimization of a Communication Satellite Multiple-Beam Antenna

A previous note [2] presented some characteristics of a communication satellite multiple-beam antenna (MBA). In this report, the configuration of such an antenna, consisting of a waveguide lens with a cluster of feeds in its focal plane, is optimized using computer modeling techniques [2] for two separate antenna systems. In the first system the antenna is required to radiate pencil beams to illuminate specified areas of the earth's surface. In the second system the antenna is required to radiate an earth-coverage beam with nulls in prescribed directions. The derivation of the directive gain of a waveguide lens MBA and the associated computer program are presented in the Appendix.

PART I AREA COVERAGE MBA

I. Introduction

The MBA is studied with the aim of optimizing the gain in any direction within a Field-of-View (FOV) by exciting the feed or the group of feeds that maximizes the power radiated in that direction. The minimum directive gain, G_m , that can be achieved under this condition is the parameter of interest and is derived for several feed cluster configurations. The study is carried out for a waveguide lens antenna with a flat feed cluster in its focal plane [1]. The field of view considered is an 18-degree cone which is about 0.6° larger than the angle subtended by the earth at synchronous altitude. The feed clusters studied include a triangular lattice arrangement of either 19, 31 or 37 feeds and a square lattice arrangement of 32 feeds. The circularly polarized feeds have a circular aperture of diameter equal to the spacing between feeds and are of two types (1) LES-7 type [1] and (2) unit-feed type. (These terms will be defined later.) The optimization is carried out at a

frequency of 7.5 GHz and the performance is calculated at this frequency and also at 7.25 and 7.75 GHz.

II. Optimization of Area Coverage MBA

Since the feed cluster is a periodic structure it is only necessary to calculate the minimum gain in two specific directions. Consider, for example, the triangular arrangement of 19 feeds shown in Fig. 1. Because the antenna directivity is smaller for feeds on the edge of the cluster, the basic cell of coverage considered contains the beams generated by exciting either feeds 21, 31 or 32 individually, as well as the beams generated by exciting any combination of these feeds with signals of equal amplitudes and in phase. The minimum directive gain within the FOV occurs in the direction where the three following beams have equal directive gains: (1) the beam resulting from excitation of feed 31, (2) the beam resulting from the simultaneous excitation of feeds 31 and 32, (3) the beam resulting from the simultaneous excitation of feeds 21, 31 and 32. This direction was found by trial and error calculations, and the corresponding minimum directive gain is plotted in Fig. 2 (dashed curve) as a function of feed spacing for a given lens diameter. On the periphery of the FOV a different situation exists and the directive gain is optimized by either exciting feed 21 alone or feeds 21 and 31 together. The peripheral direction where the two resulting beams have equal directive gains was again found and the corresponding directive gain is plotted as the solid curve in Fig. 2. For a given lens diameter and feed spacing the minimum directive gain, G_m , over the entire FOV is the lesser of the two values read from either the solid or the dashed curves in Fig. 2. The intersection of the

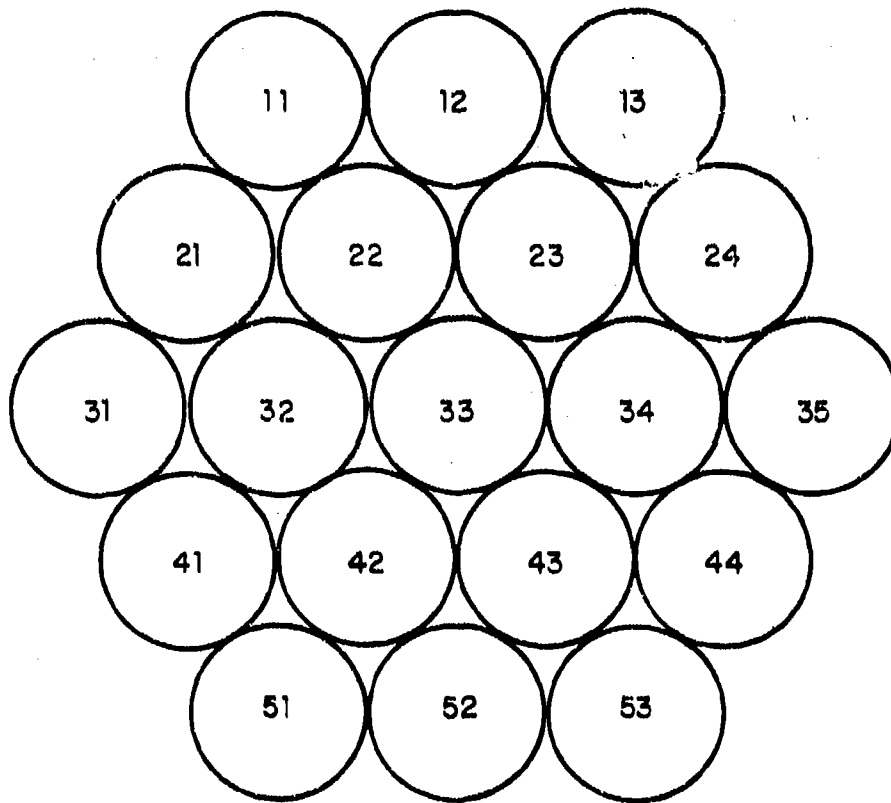


Fig. 1. Feed arrangement.

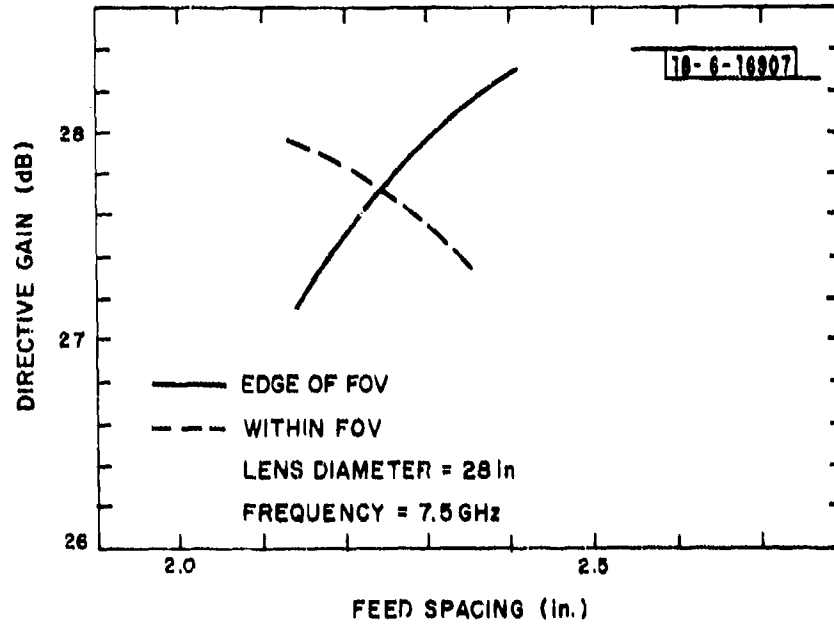


Fig. 2. Directive gain vs feed spacing for a given lens diameter.

two curves determines the maximum value of G_m , and the corresponding optimum separation between feeds. The values of G_m for other lens diameters, and feed spacings are given by the bottom curve in Fig. 3. Note that G_m is not strongly dependent on lens diameter between 24 inches and 34 inches, for which G_m remains within 0.3 dB of its peak value.

The above result is achieved with in-phase excitation of feed combinations. However, since the feeds are coplanar, the phase of the far field arising from excitation of an offset feed is delayed with respect to that of the center feed by an amount increasing with feed offset angle. The directivities of beams resulting from multiple feed excitations are somewhat reduced by this effect. The phase delays could be removed by locating the feeds on a spherical cap whose geometric center is at the vertex of the lens inner surface or by exciting each feed with a signal whose phase is advanced by an amount equal to its relative delay (phase correction). This latter method was studied with the result depicted by the dashed curve of Fig. 3 indicating that phase correction leads to an increase of about 0.3 dB for G_m .

The minimum directivity curves of Fig. 3 apply to a cluster of 19 circular horns excited with a TE_{11} mode (LES-7 type feeds). The aperture efficiency of this feed is about 83.5% and the area of its aperture is 91% of the maximum available area per feed, called a "unit cell" area. A unit feed is defined as a feed whose uniformly illuminated aperture is that of the unit cell. The gain of a unit feed is thus 1.2 dB larger than the gain of a LES-7 type feed. It is believed that practical feeds may be realized whose gain (within the feed cluster environment) is equal to but not greater than that of the unit feed. One possible technique of achieving this, for example, is by the addition of a polyrod in the aperture of a horn. Another technique is to divide

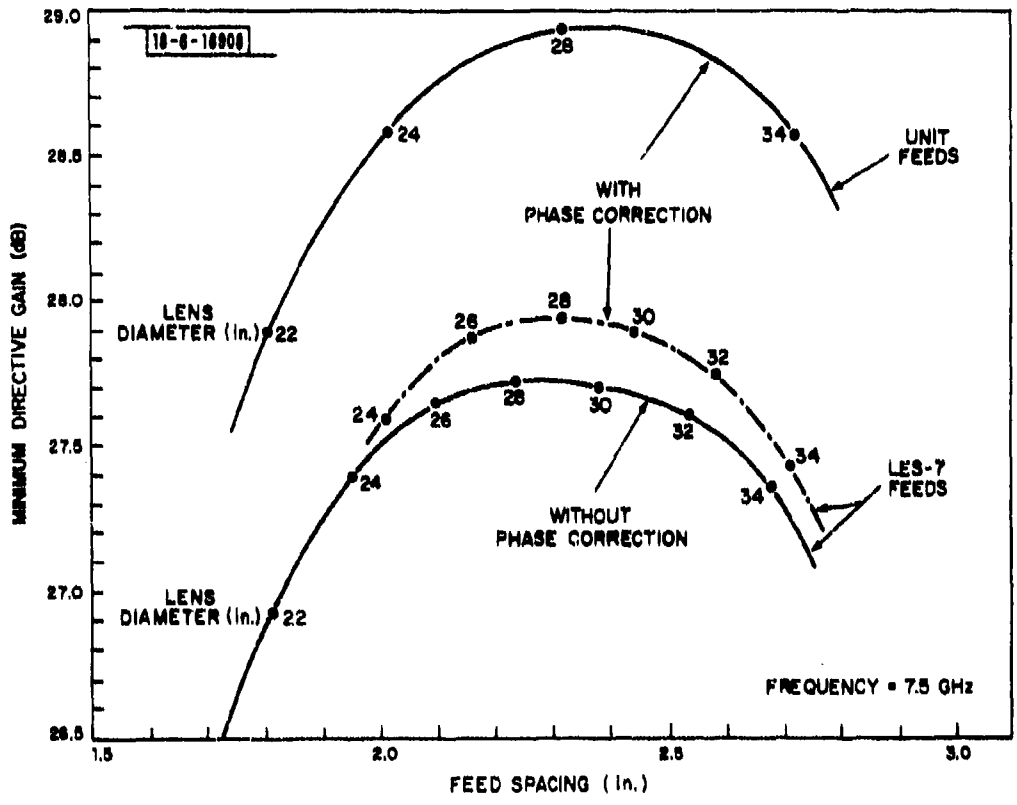


Fig. 3. Directive gain vs feed spacing for different lens diameters.

the feed horn aperture into several smaller apertures of dimension less than a free-space wavelength by means of metal septa. This latter technique has proved practical with square aperture horns. The minimum directive gain of a waveguide lens MBA, embodying a cluster of 19 triangularly spaced unit feeds, was calculated for the case where the feeds are excited with phase-corrected signals. The results are shown in Fig. 3 (top curve). The radiation pattern of the unit feed, intrinsic in the calculation, is the function $2J_1(u)/u$ with $u = (2\pi a/\lambda)\sin\theta$ where θ is the angle from the axis of the unit feed and a is the radius of a circular aperture of area equal to that of the unit feed. Figure 3 shows that the peak value of 28.9 dB for G_m is obtained with a lens diameter of about 28 inches and a feed spacing of about 2.31 inches. The radiation patterns for this optimum configuration, when each feed of the center row is excited individually, are presented in Fig. 4. The peak directivity of 31.9 dB corresponds to an aperture efficiency of 50%. The half-power beamwidth of each beam is 3.6° , the crossover level is about 5 dB below the peak directivity and the edge beam is seen to point very near the boundary of the FOV. The beams formed by exciting two or three adjacent feeds together are typified by the contour plots of Fig. 5 where 3 beams are shown: (1) the beam resulting from excitation of feed 31 has a circular cross section with directivity of 31.3 dB, (2) the beam resulting from excitation of feeds 31 and 32 has an elliptic cross section with directivity of 29.6 dB, (3) the beam resulting from excitation of feeds 31, 32 and 21 has a "triangular" cross section with directivity of 29.4 dB. The directive gain in dB is shown on each contour; levels below 27 dB are not shown for clarity. It is observed that the directive gain of each of the three beams is equal to the minimum value of

19-BEAM WAVEGUIDE LENS ANTENNA
CIRCULAR POLARIZATION
UNIT FEEDS
PHASE CORRECTED
PEAK GAIN = 31.89 dB

LENS DIAM = 28 in.
DESIGN FREQUENCY = 7.5 GHz
FEED SPACING = 2.31 in.
FREQUENCY = 7.5 GHz
F/D = 1
PLANE OF PATTERN CUT = 90 deg

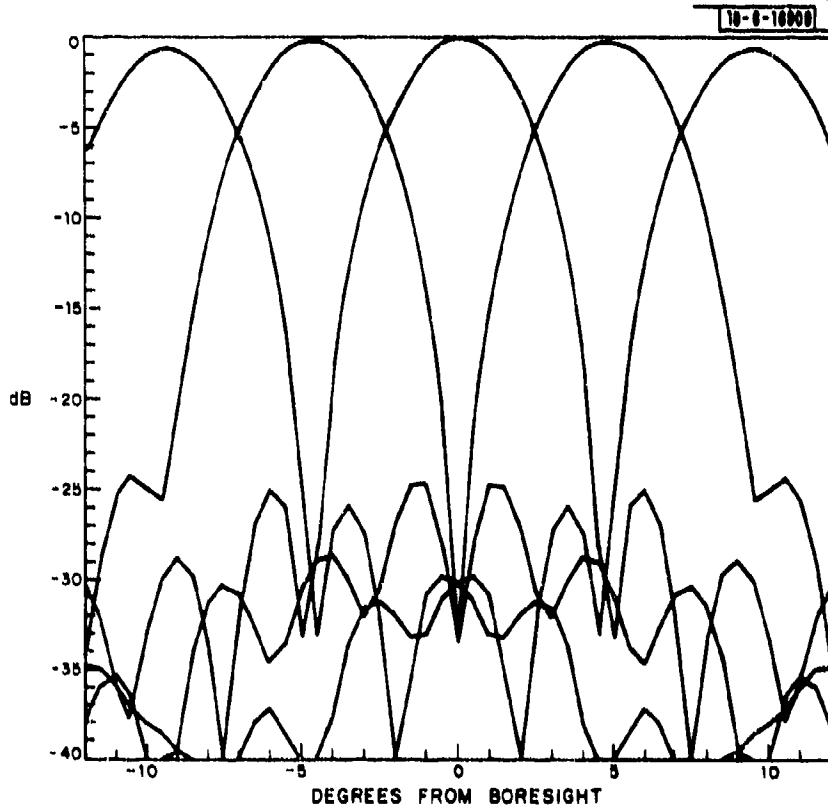


Fig. 4. Superimposed beams of center row.

19-BEAM WAVEGUIDE LENS ANTENNA
CIRCULAR POLARIZATION
UNIT FEEDS
PHASE CORRECTED
LENS DIAM = 28 in.

DESIGN FREQUENCY = 7.5 GHz
FEED SPACING = 2.32 in.
FREQUENCY = 7.5 GHz
F/D = 1

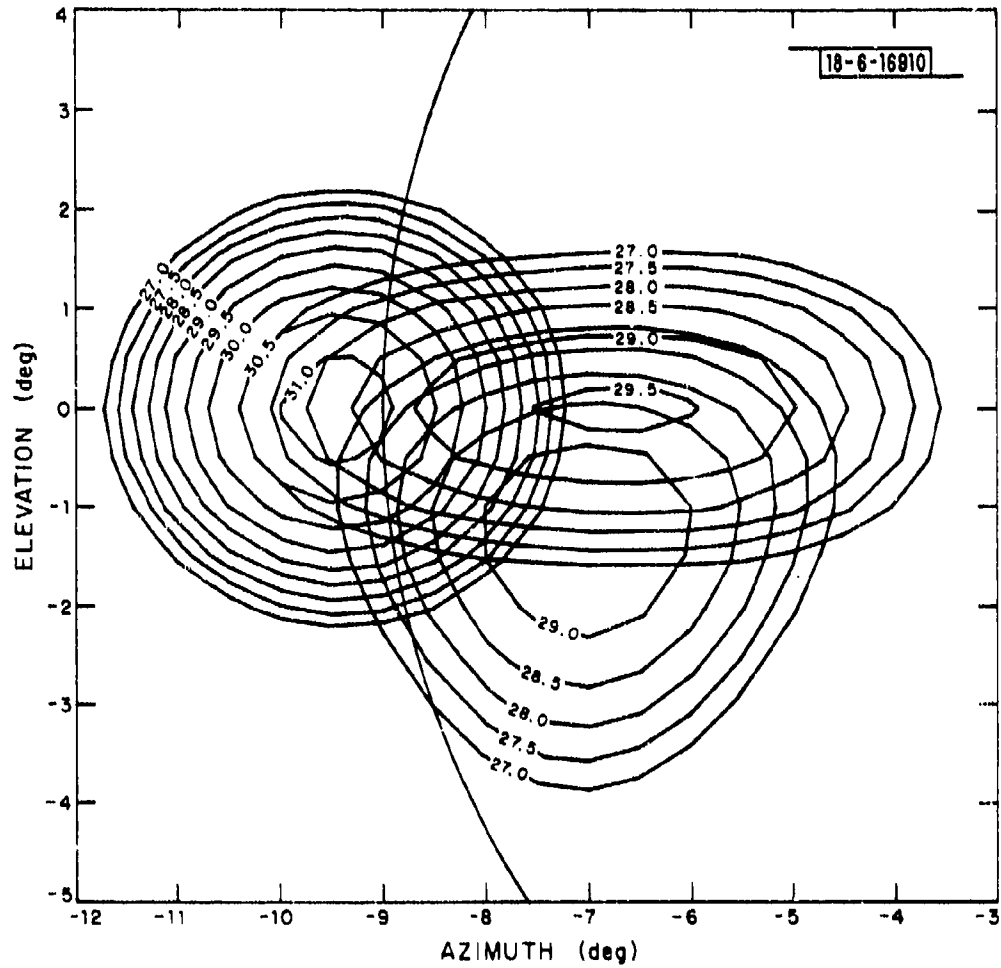


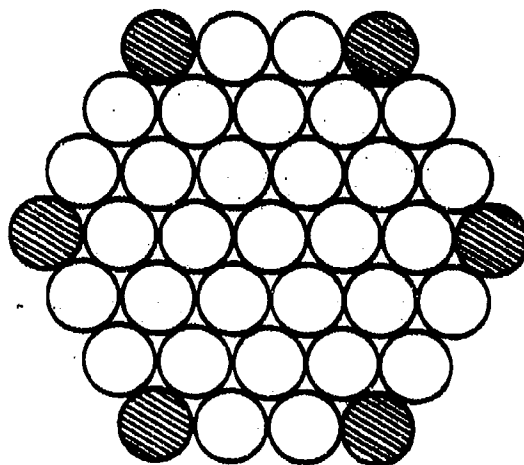
Fig. 5. Contour plot of three typical beams.

of about 28.9 dB (G_m) in the direction $AZ = 8^\circ$, $EL = -0.75^\circ$.

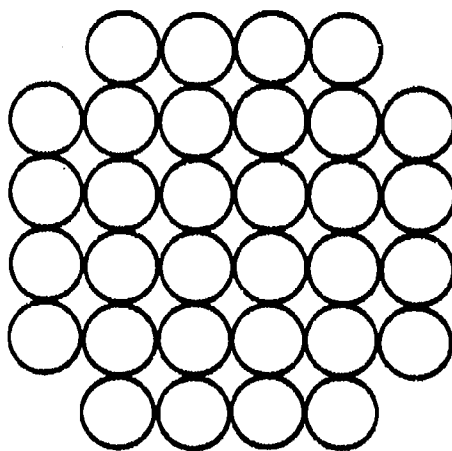
In addition to the cluster of 19 feeds, clusters of 31 feeds and of 37 feeds were also studied. The 31-feed cluster is the 37-feed cluster with the six outermost feeds removed as shown in Fig. 6a. Also studied was a 32-feed cluster on a square lattice as shown in Fig. 6b. In this latter case either one, two or four adjacent feeds are excited to provide the coverage. The comparative performance of the different feed clusters is presented in Fig. 7 as a function of lens diameter. The corresponding optimum feed spacing is plotted in Fig. 8.

III. Beam Steering

The minimum directive gain previously derived implies that a finite number of beams pointing in discrete directions within the FOV are generated. A number of these beams are produced by exciting two or three adjacent feeds in which case, equal signals are fed to each feed. However, the beam-forming network postulated[2] allows any power division among the feeds, making possible continuous beam steering between the beam directions of the singly excited feeds. With beam steering, the minimum directive gain of the MBA is increased as compared to the simpler case described in Section II. The characteristics of the beam formed by fractional excitation of two adjacent feeds are typified by Fig. 9 which shows the directive gain and pointing direction of such a beam as a function of the fractional power delivered to feeds 32 and 33. An example of a case where three adjacent feeds are excited fractionally is given in Fig. 10 which shows a beam pointing close to the previously de-



(a)



(b)

Fig. 6. Clusters of (a) 37 feeds and (b) 32 feeds.

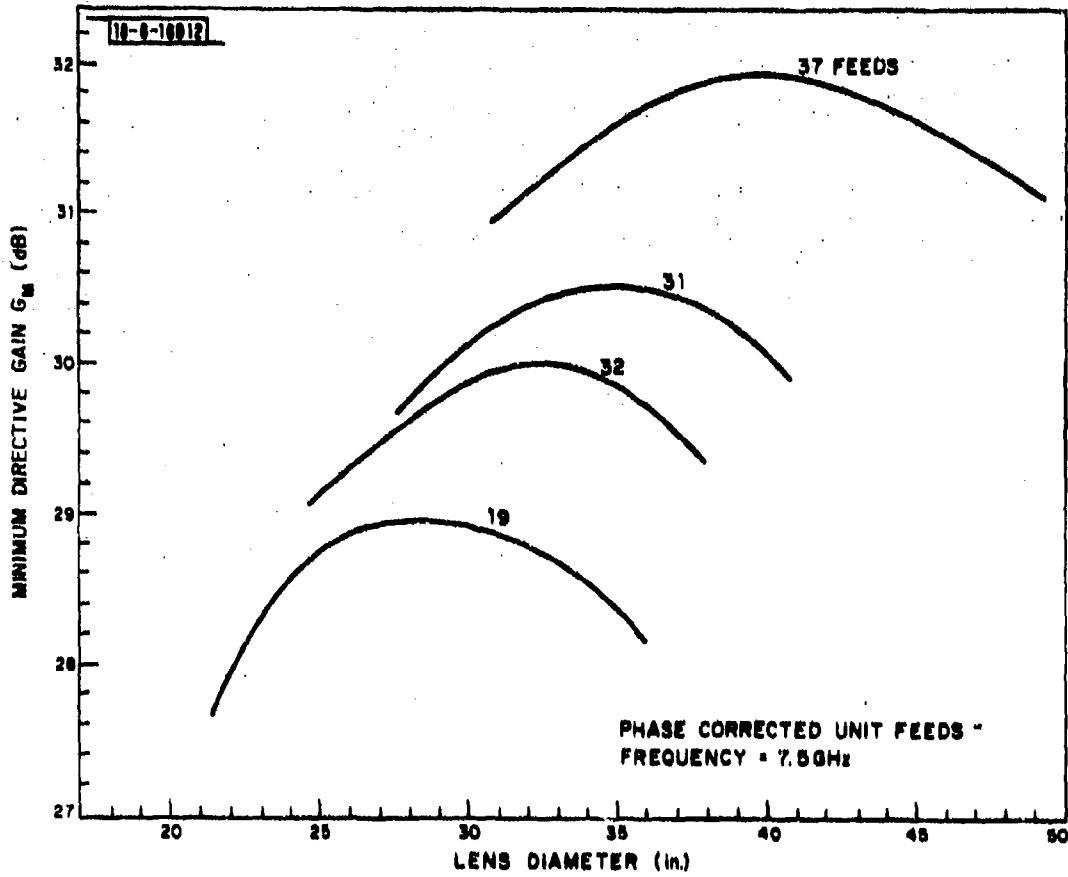


Fig. 7. Optimum performance curves of area-coverage MBA.

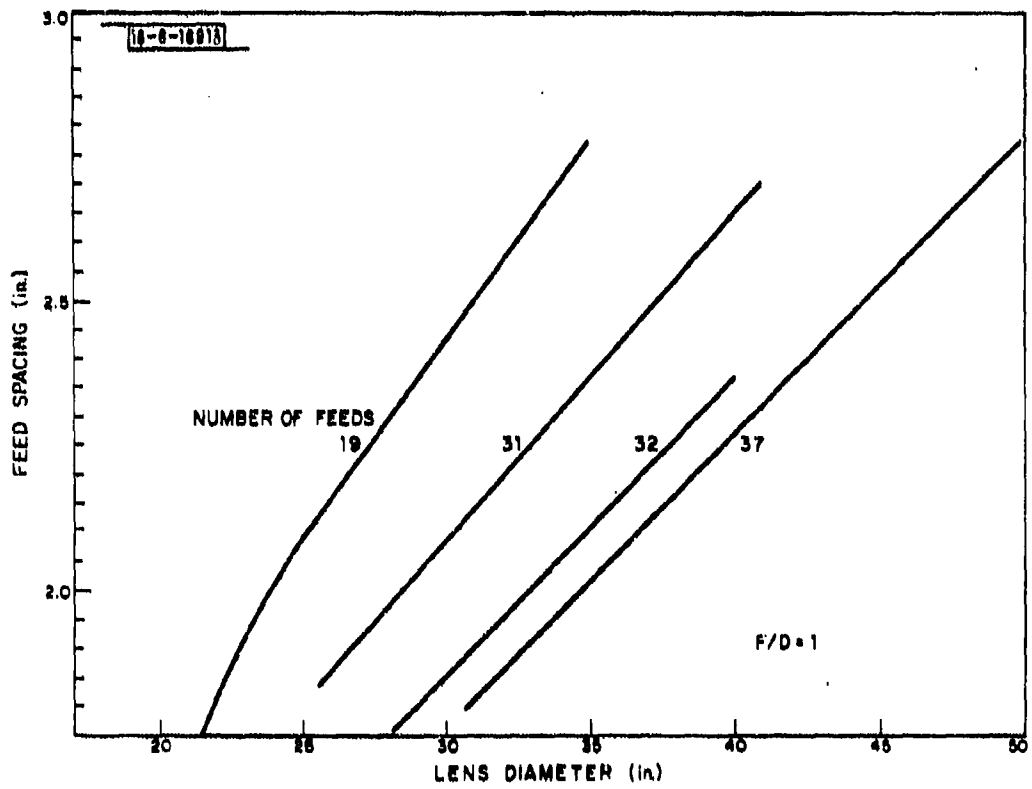


Fig. 8. Optimum feed spacing vs lens diameter of area-coverage MBA.

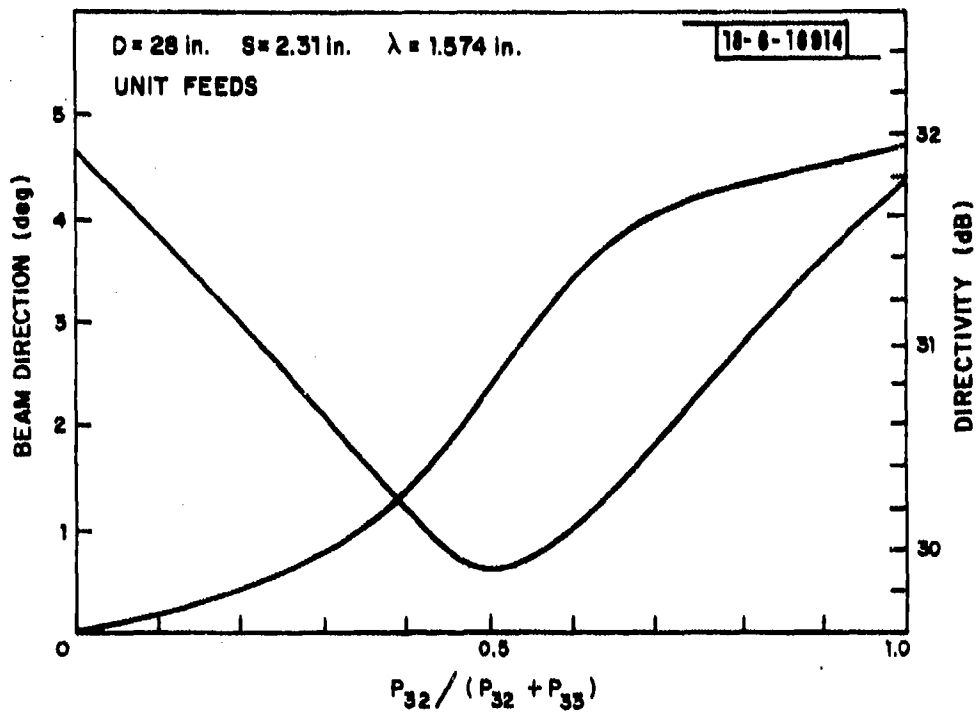


Fig. 9. Directivity and beam direction of steered beam.

19-BEAM WAVEGUIDE LENS ANTENNA
CIRCULAR POLARIZATION
UNIT FEEDS
PHASE CORRECTED
DIRECTIVITY = 29.56 dB

LENS DIAM = 28 in.
DESIGN FREQUENCY = 7.5 GHz
FEED SPACING = 2.32 in.
FREQUENCY = 7.5 GHz
F/D = 1

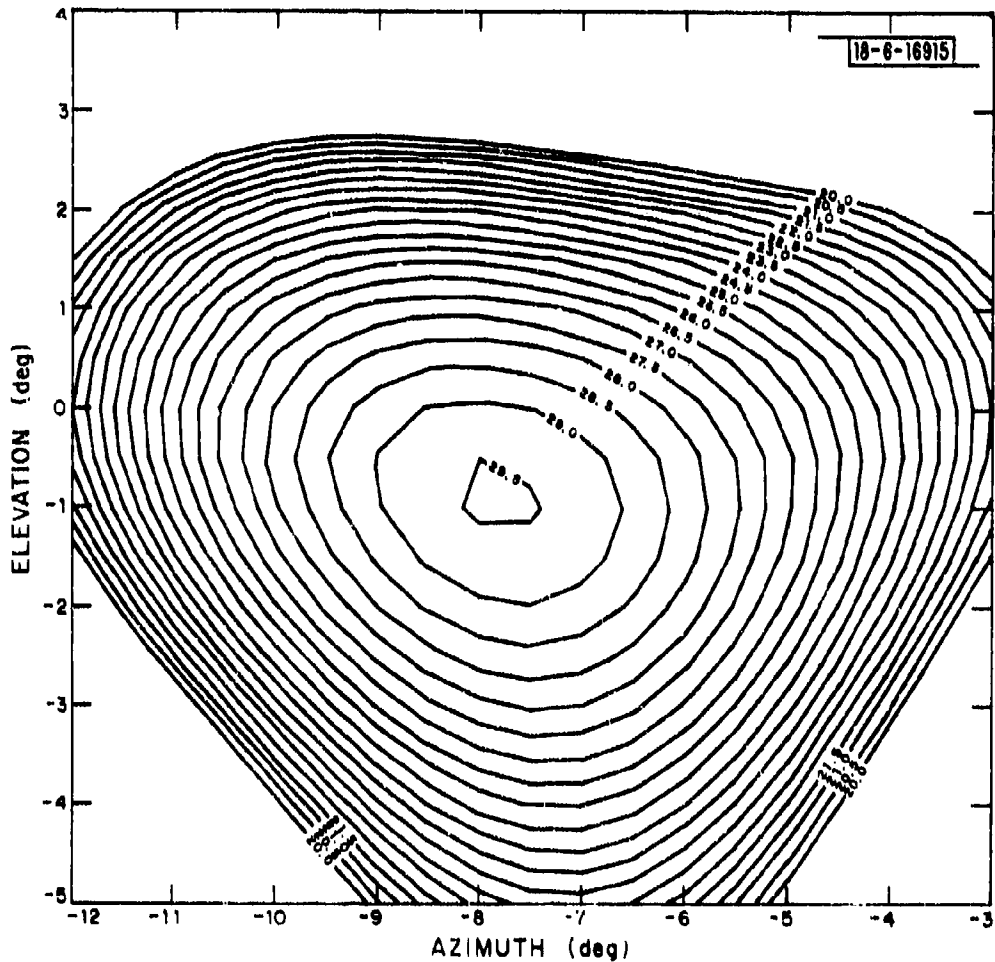


Fig. 10. Contour plot of a steered beam.

rived minimum-directive-gain direction (i.e., $AZ = -8^\circ$, $EL = -0.75^\circ$), a result obtained by exciting feeds 21, 31 and 32 with power ratios equal to 0.25, 0.50 and 0.25, respectively. The antenna configuration in each of the above two cases is the optimum 19-feed waveguide lens MBA. Clearly, beam steering can only raise the minimum directive gain to the directivity of the beam formed when three adjacent feeds are fed equally and in phase, and for the present case this value is 29.4 dB.

IV. Frequency Behavior

The waveguide lens MBA was optimized for a frequency of 7.5 GHz. The effect of frequency on the performance of the 19-feed optimum configuration is shown in Fig. 11 over the range 7.25 GHz to 7.75 GHz. It is observed that at 7.25 GHz the minimum directive gain drops about 0.7 dB. This drop is due mostly to dispersion by the waveguide lens as evidenced by the dashed curves which show the calculated performance when the lens dispersion factor is removed. (The dispersion factor was removed by calculating a new perfect lens at each frequency.)

V. Effect of F/D Ratio

The directivity of the center beam (feed 33 excited) of the 19-feed optimum MBA is plotted in Fig. 12 as a function of the F/D ratio. Two waveguide lenses were considered (1) a waveguide lens with a spherical inner surface of radius equal to the focal length and (2) a waveguide lens with inner surface of radius equal to the lens diameter. The sharp drops of about 0.5 dB occur for values of F/D at which zoning takes place. The performance of the waveguide lens as a function of F/D reflects principally the effects of two

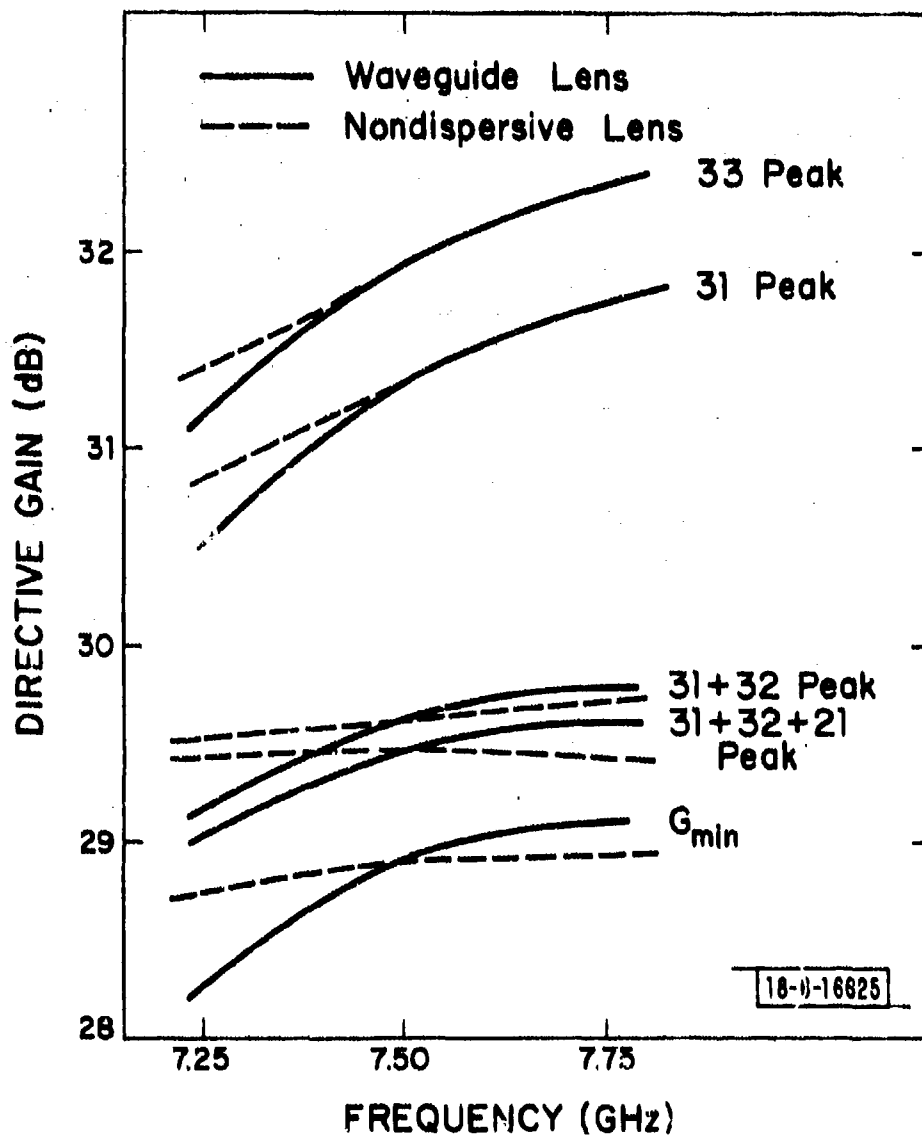


Fig. 11. Directive gain as a function of frequency.

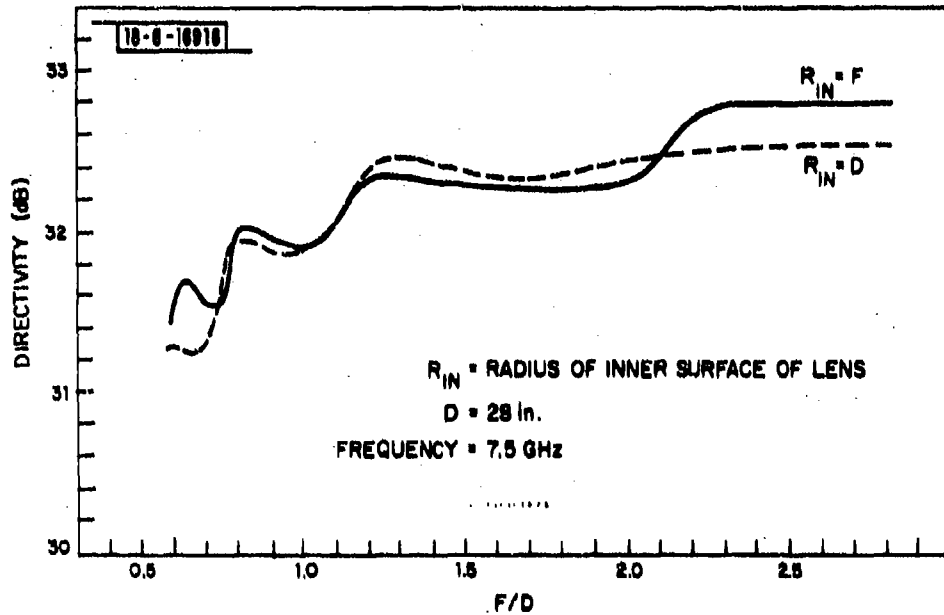


Fig. 12. Directivity of center beam as a function of F/D ratio.

assumptions inherent to the calculations. The first one is the absorbing pattern of the waveguide elements of the lens which is assumed to be a $\cos\theta$ pattern pointing toward the geometric center of the inner surface of the lens and the second one is the assumed radiation pattern of waveguide elements adjacent to steps in the lens. The validity of these assumptions is substantiated in part by the good agreement between the measured and calculated directive gains of the LES-7 MBA which has an F/D ratio equal to unity. However, as this ratio decreases, the validity of the first assumption becomes increasingly dubious, yielding lesser confidence in the corresponding results.

VI. Tolerances on Power Divider

Multiple-beam antennas with triangularly spaced feed clusters require excitation of up to three feeds with in-phase signals of equal power levels. Deviations from the in-phase condition cause a decrease of the directivity of the resulting beam with a corresponding decrease of G_m . A phase error of $\pm 20^\circ$ between input signals yields a reduction of 0.12 dB of the minimum directive gain. Non-uniform excitation of the feeds causes a squint of the beam and a reduction of G_m . For a deviation of ± 1 dB the calculated reduction of G_m is 0.15 dB. Thus the effect of even appreciable deviations from uniform phase and amplitude excitation is negligible.

PART II EARTH COVERAGE WITH PRESCRIBED NULLS MBA

I. Introduction

The characteristics of a multiple-beam antenna designed to radiate an earth-coverage beam with nulls in prescribed directions are investigated in this Part. The MBA considered consists of a waveguide lens with a cluster of 19 feeds in its focal plane. The MBA dimensions are chosen to optimize the minimum value of directive gain over a cone angle of 18° and also to maximize the depth of the null (an appreciable reduction of gain in a prescribed direction is termed a null) produced when one feed of the feed cluster is not excited. Optimization is carried out at the center frequency of a 7.9 to 8.4 GHz frequency band. The predicted performance of the optimum configuration at the center frequency and at the extreme frequencies of this band is presented as well as the calculated performance degradation caused by errors in the feed excitation coefficients. The 19-feed MBA nulling antenna allows one to reduce the gain by at least 15 dB in any direction over the FOV by suppressing excitation to either a single feed or to a group of two or three adjacent feeds. The disadvantage of this nulling technique is that by suppressing excitation to a group of adjacent feeds the gain reduction occurs over an undesirably large area. However, by means of a null steering technique it is possible to direct a null, of coverage about equal to that obtained by suppressing excitation to a single feed, toward any directions over the FOV. To implement the null steering technique, however, a tight control of phase is required. The disadvantages of the former two techniques are eliminated by increasing the quantity of feeds in the cluster. The performance of a 61-feed cluster is

presented and shown to offer distinct advantages. The disadvantage of this latter configuration is, of course, the much larger feed network required.

II. Optimization of Nulling MBA

The waveguide lens and feed cluster optimized is the LES-7 configuration with the exception that a cluster of unit feeds is considered. Optimization is carried out as follows: For a given lens diameter and with the feed spacing as a variable parameter the directive gain is calculated for an appropriate number of directions within an element of symmetry of the FOV. The feeds are all excited equally (except as described next) and their phase is adjusted to produce spherical wavefront secondary radiation (phase corrected). For small values of feed spacing, the lowest directive gain is found to occur within the FOV at the bottom of the ripple superimposed on a nearly flat pattern. The feed spacing which optimizes the minimum value of the Earth-Coverage directive Gain (ECG_{MIN}) is that value s_0 which makes the minimum gain within the FOV, and that along the boundary, equal. This optimum value was calculated first with all feeds excited equally. By exciting the feeds such as to produce a more uniform directive gain around the periphery of the FOV a larger value of ECG_{MIN} can be reached. The boundary of the feed cluster is a hexagon and therefore with the feeds equally excited the radiation pattern is broader in planes passing through the corner of this hexagon than in bisecting planes. Therefore, exciting the corner feeds with less power than intermediate feeds along the periphery, will make the directive gain more uniform along the boundary of the FOV and will lead to a slightly larger

ECG_{MIN} . Thus the above optimization procedure was also carried out for different values of the power excitation ratio r , i.e., the ratio between the power fed to corner feeds and that fed to intermediate feeds, and the value r_0 which maximizes ECG_{MIN} was determined. This procedure repeated for an appropriate range of lens diameter yielded the results represented by the solid curve of Fig. 13. The minimum directive gain over the FOV peaks at about 19.3 dB and is at least 19 dB for lens diameter of 22 to 32 inches. The dip in the curve at a diameter of about 26 inches is believed to be caused by an additional zoning step, since lenses with diameter larger than 26 inches contain one zone more than the smaller diameter lenses.

The next step in optimizing the nulling MBA is to determine the depth of the null produced by suppressing excitation to one feed of the optimum configuration. The dashed curve of Fig. 13 shows the results obtained when feed 32 is not excited. The largest null depth is reached with a lens diameter of 28 inches for which the null level is -17 dBi, i.e., about 36 dB below the minimum directive gain. The optimum values of the feed spacing and of the power excitation ratio are plotted in Fig. 14 as a function of the lens diameter.

The contour plot of the earth-coverage beam obtained with the optimum configuration, i.e., a lens diameter of 28 inches, a feed spacing (s_0) of 2.35 inch and a power excitation ratio (r_0) of -0.83 dB is given in Fig. 15. The peak directive gain is 20.8 dB and the minimum directive gain over the FOV is 19.3 dB. Figure 16 shows the coverage obtained with excitation of feed 32 suppressed and Fig. 17 shows a typical case of null steering obtained by setting the phase of the signals to feeds 32 and 33, -90° and $+90^\circ$, respectively, as compared to the phase of the signals to all other feeds. Inspection of the narrow beams

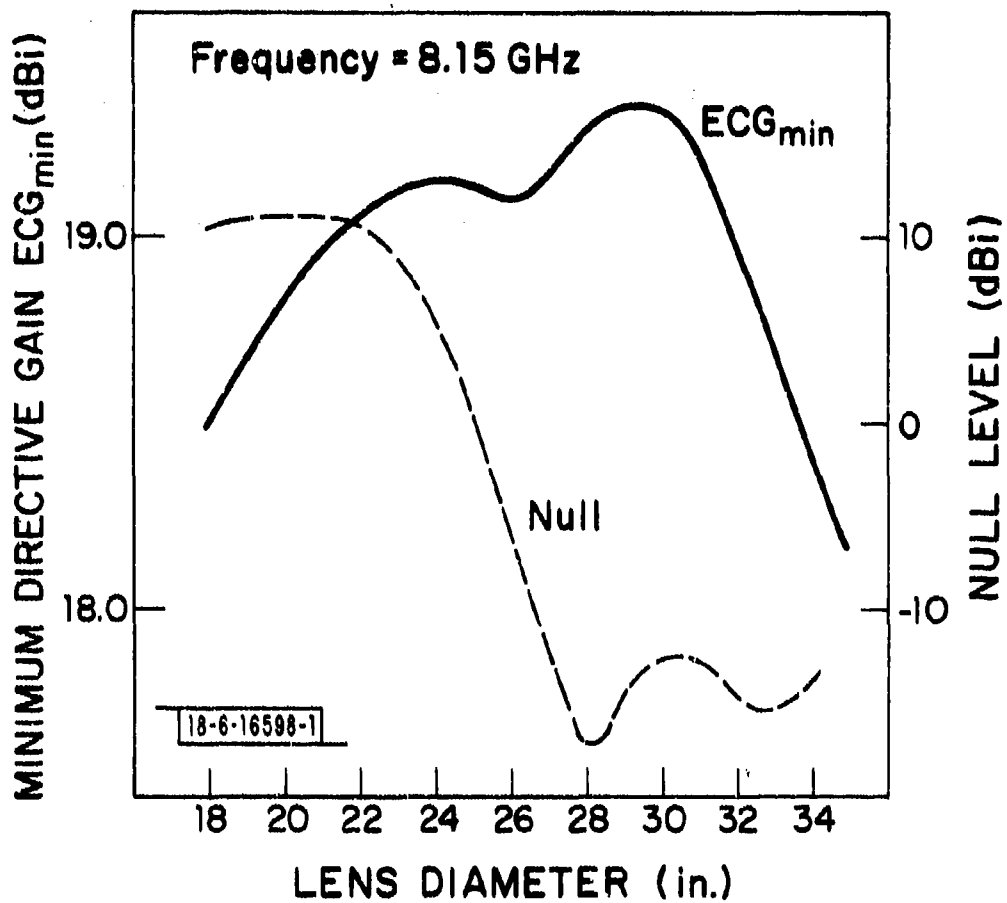


Fig. 13. Optimum performance of earth-coverage MBA.

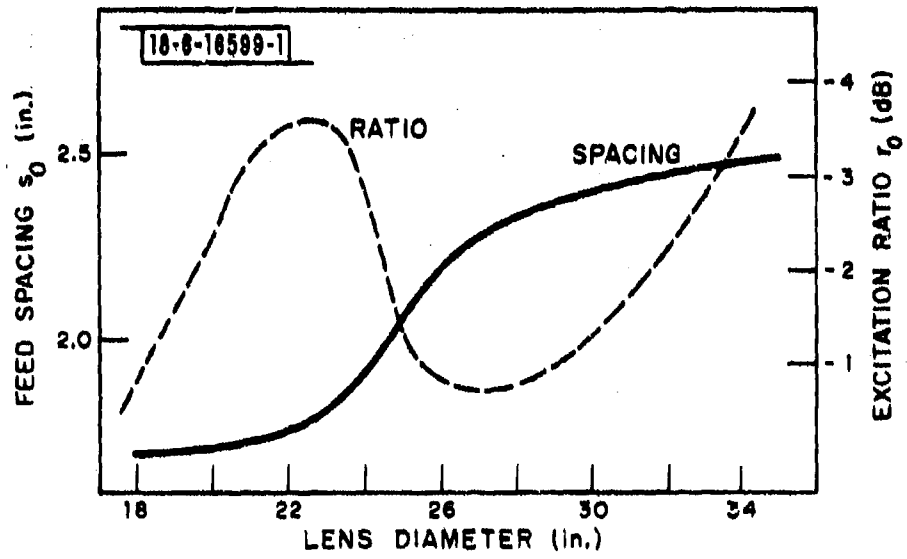


Fig. 14. Optimum feed spacing and excitation ratio of earth-coverage MBA.

19-BEAM WAVEGUIDE LENS ANTENNA
CIRCULAR POLARIZATION
UNIT FEEDS
PHASE CORRECTED
DIRECTIVITY = 20.85 dB
LENS DIAM = 28 in.

DESIGN FREQUENCY = 6.15 GHz
EXCITATION RATIO = -0.83 dB
FEED SPACING = 2.35 in.
FREQUENCY = 8.15 GHz
F/D = 1

-6-16606-1

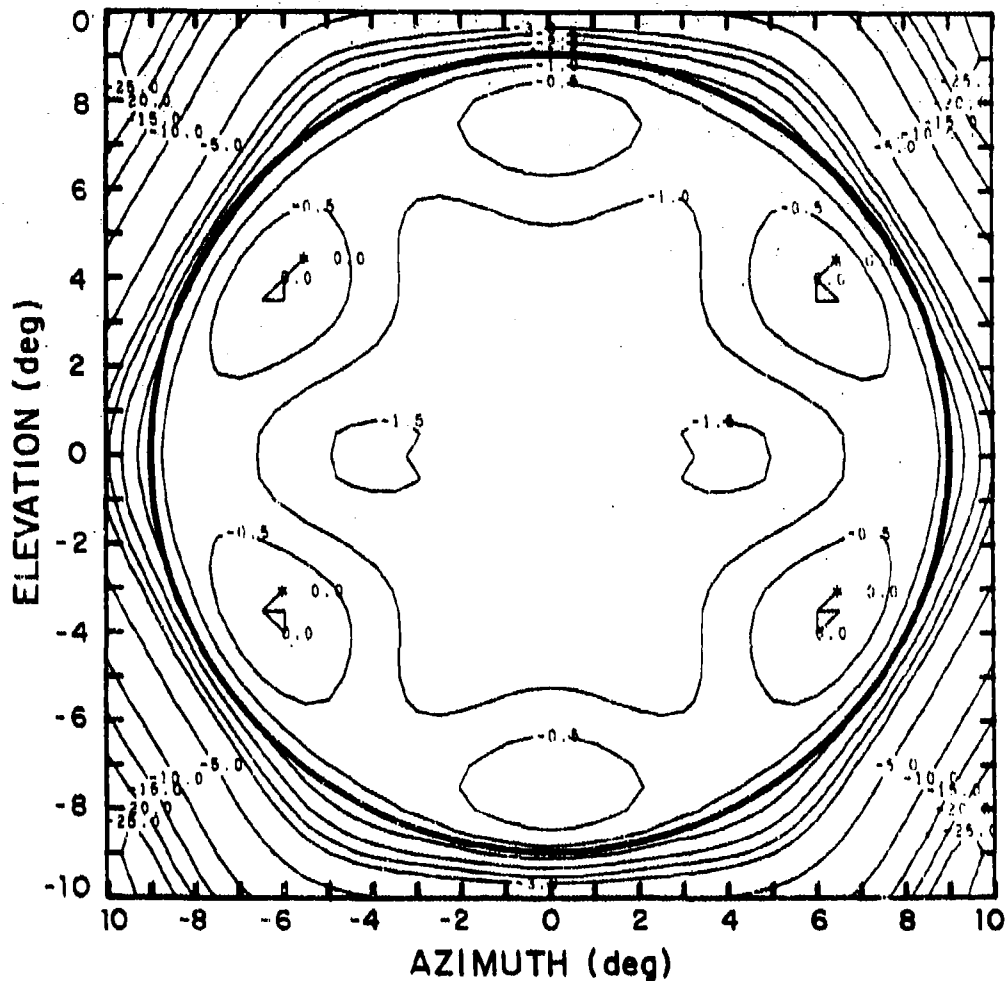


Fig. 15. Contour plot of optimally designed earth-coverage MBA.

19-BEAM WAVEGUIDE LENS ANTENNA
CIRCULAR POLARIZATION
UNIT FEEDS
PHASE CORRECTED
ALL FEEDS EXCITED EXCEPT 3, 2
DIRECTIVITY = 21.25 dB

LENS DIAM = 28 in.
DESIGN FREQUENCY = 8.15 GHz
EXCITATION RATIO = -0.83 dB
FEED SPACING = 2.35 in.
FREQUENCY = 8.15 GHz
F/D = 1

-6-16605-1

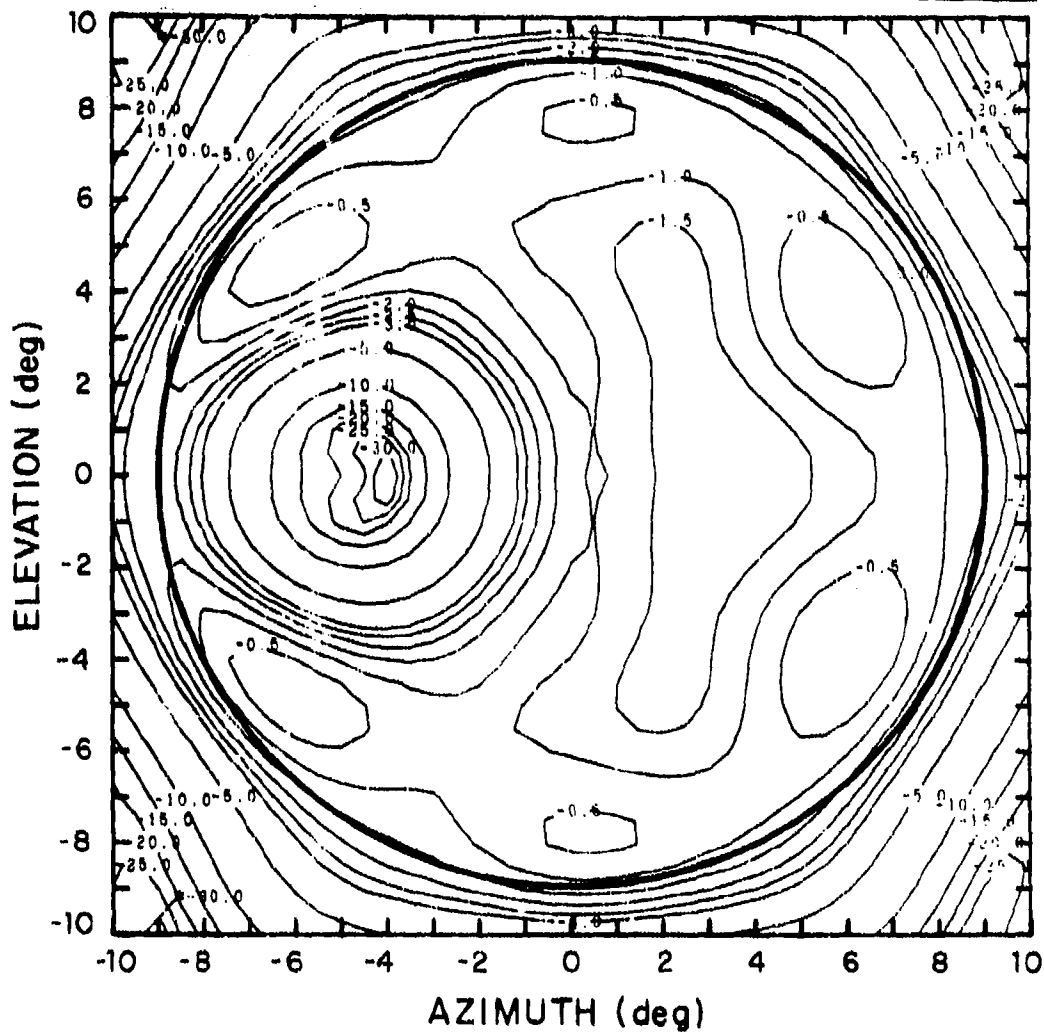


Fig. 16. Contour plot of earth-coverage MBA with excitation to one feed suppressed.

19-BEAM WAVEGUIDE LENS ANTENNA
CIRCULAR POLARIZATION
UNIT FEEDS
PHASE CORRECTED
DIRECTIVITY = 21.17 dB
LENS DIAM = 28 in.
DESIGN FREQUENCY = 8.15 GHz

EXCITATION RATIO = -0.83 dB
FEED SPACING = 2.35 in.
FREQUENCY = 8.15 GHz
F/D = 1
PHASE (3,2) = -90 deg
PHASE (3,3) = 90 deg

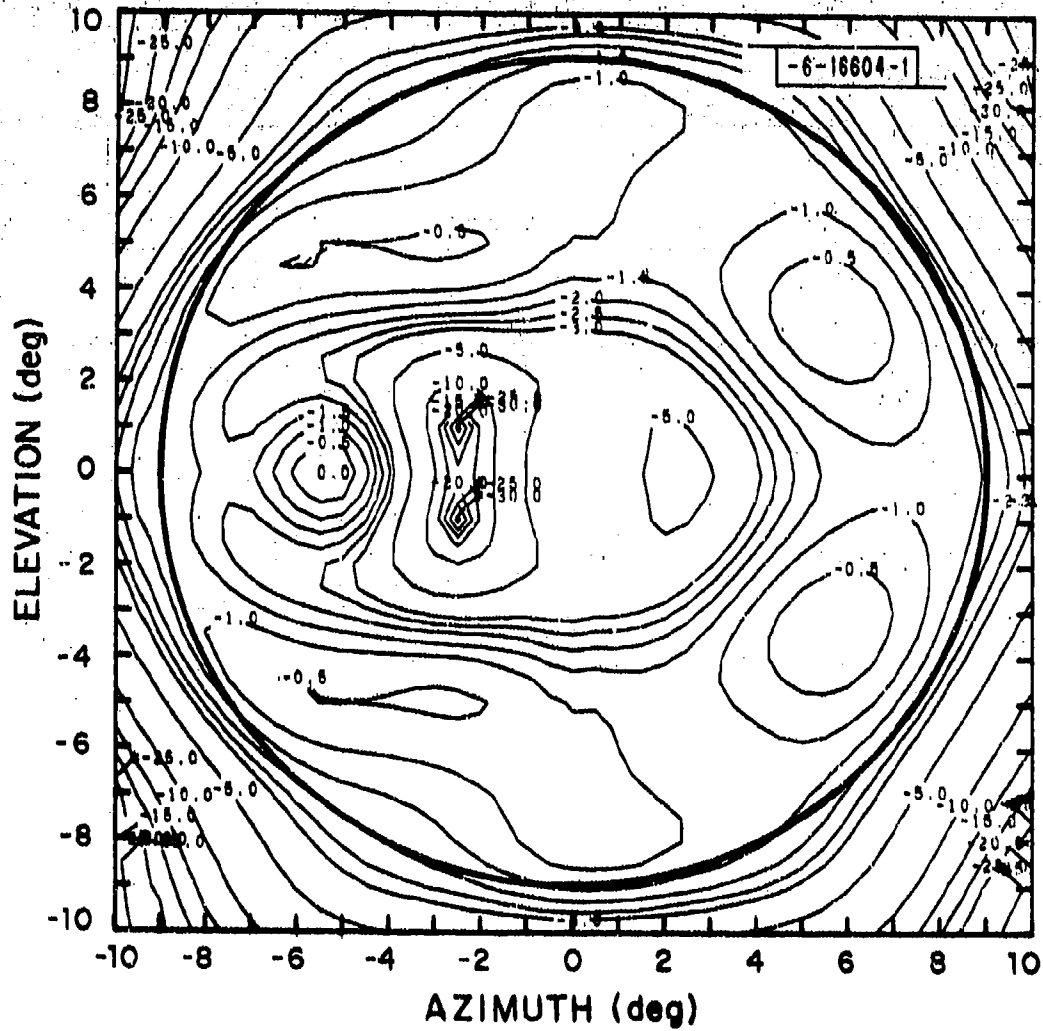


Fig. 17. Contour plot of a steered null.

generated when each feed of the optimum configuration is excited alone (see Fig. 3 which applies to a similar configuration except for the feed spacing which is equal to 2.31 in.) shows that, as anticipated, the beams are nearly orthogonal, i.e., in the direction of the peak of any beam the amplitude of the radiation from the other beams is close to a minimum. Thus deep nulls in an earth-coverage beam are associated with low-minima narrow beam patterns.

The characteristics of a 26-inch waveguide lens with a 19-feed cluster were reported by Ricardi, et al. [2] This configuration though not optimized to produce the deepest null was verified to lead to 15-dB gain reduction contours nearly identical to those of the optimum configuration.

III. Frequency Behavior

The effect of frequency on the earth-coverage beam is slight as illustrated in Fig. 18 by the patterns computed at the center and extreme frequencies of a 500-MHz bandwidth. The effect of frequency on the depth of null is severe, however, as shown in Fig. 19 by the patterns passing through the minimum of the null at five frequencies over the same bandwidth. This behavior was not unexpected since the waveguide lens is dispersive and the primary effect of dispersion is to raise the level of the minima in the patterns associated with single-feed excitation and hence reduce the null depth achievable. That the lens dispersion is the primary cause of the observed drastic reduction of null depth is demonstrated by the results obtained when the waveguide lens is replaced by a non-dispersive lens (Fig. 20). In this case the null depth is seen to remain greater than 30 dB and the null width at a depth of 15 dB is constant over the band.

DIAM = 28 in.
F/D = 1
SPACING = 2.35 in.
LENS DESIGN FREQUENCY = 8.15 GHz

PLANE OF PATTERN CUT = 90 deg
MAXIMUM DIRECTIVITY = 20.41 dB
19-BEAM WAVEGUIDE LENS ANTENNA
CIRCULAR POLARIZATION

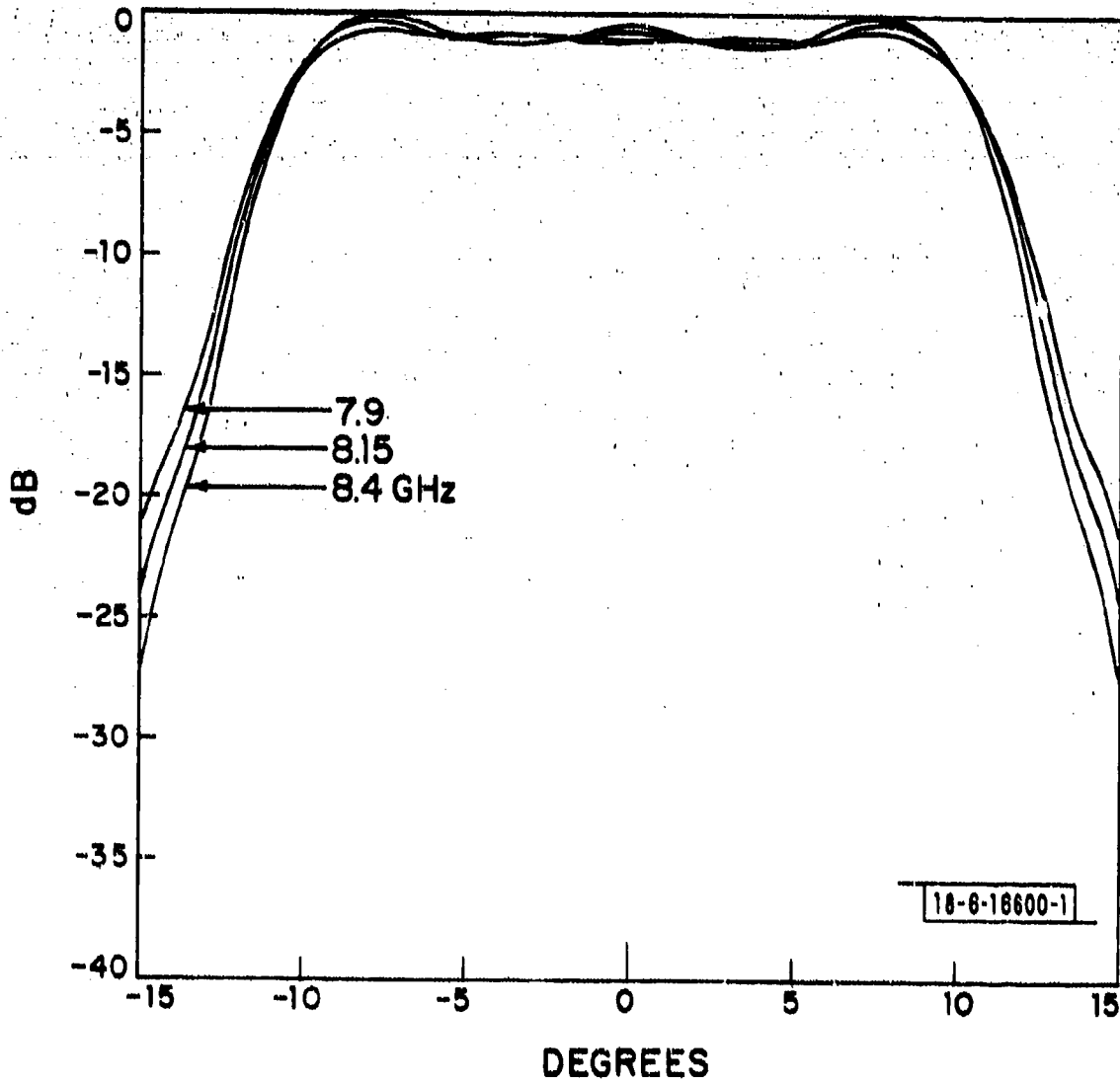


Fig. 18. Effect of frequency on earth-coverage beam.

DIAM = 28 in.
F/D = 1
SPACING = 2.35 in.
LENS DESIGN FREQUENCY = 8.15 GHz

PLANE OF PATTERN CUT = 90 deg
DIRECTIVITY = 20.69 dB
19-BEAM WAVEGUIDE LENS ANTENNA
CIRCULAR POLARIZATION

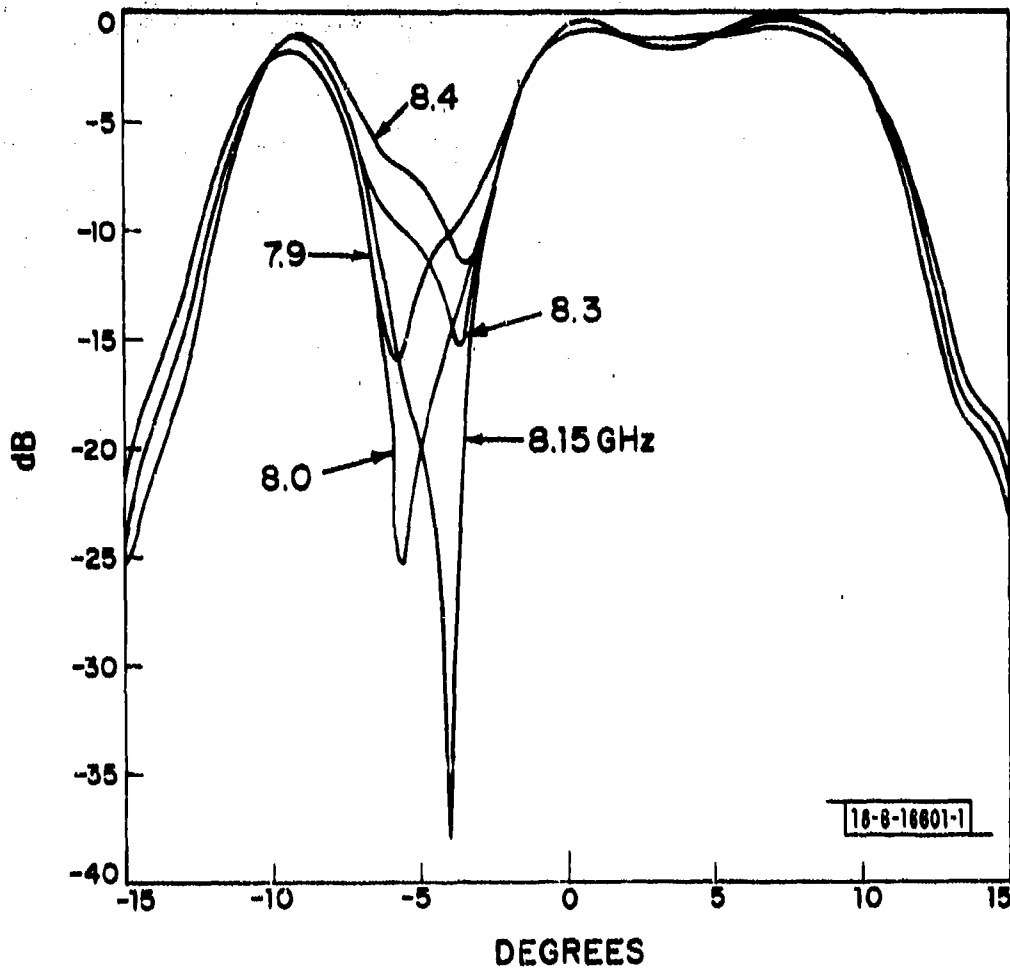


Fig. 19. Effect of frequency on the null produced by suppressing excitation of feed 32.

DIAM = 28 in.
F/D = 1
SPACING = 2.35 in.
PLANE OF PATTERN = 90 deg

DIRECTIVITY = 20.80 dB
19-BEAM NONDISPERSIVE LENS ANTENNA
CIRCULAR POLARIZATION

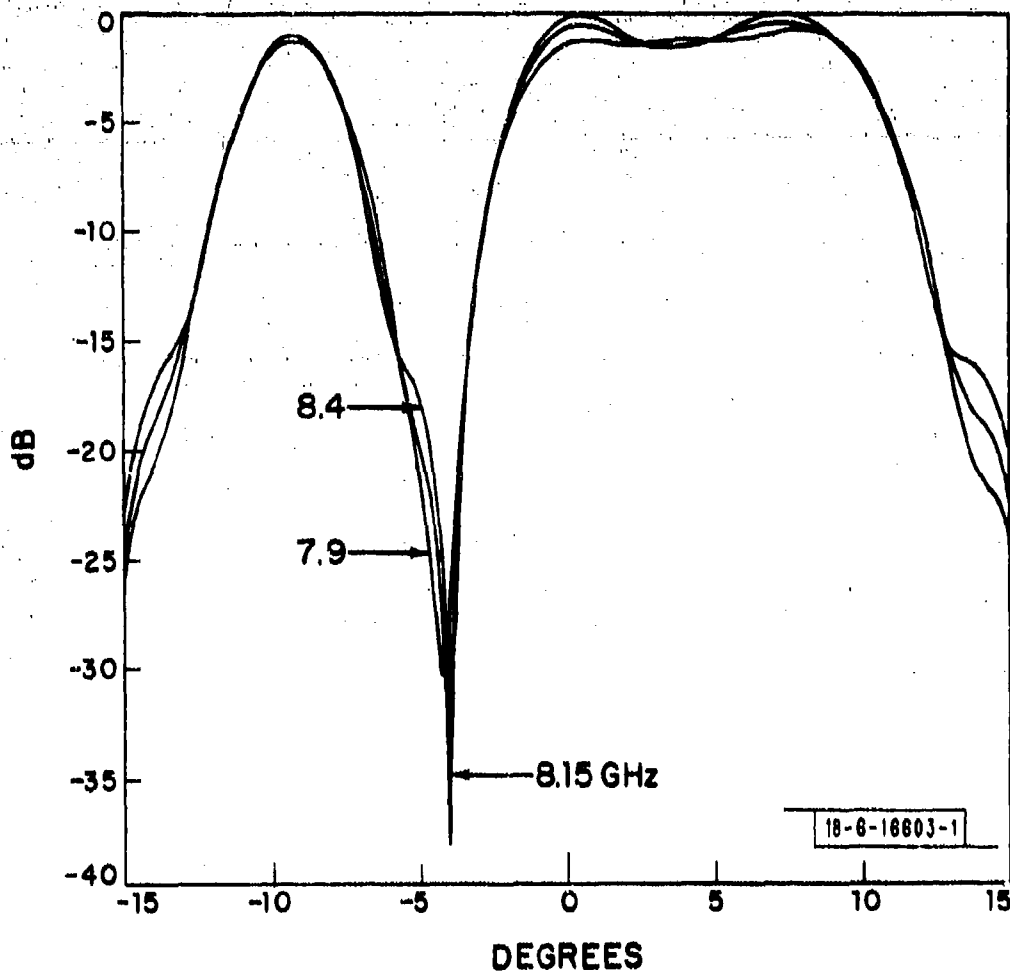


Fig. 20. Effect of frequency on the null of Fig. 19 for an MBA with a non-dispersive lens.

IV. Effect of Errors on Feed Excitation Coefficients

The effect on performance of errors on the amplitude and phase of the signals applied to the feeds was determined by computing the radiation characteristics of the optimum configuration when errors are added to the required signals. Normal distributions of errors with a 3σ power deviation equal to 0.5 dB and a 3σ phase deviation equal to 15° were chosen. Calculations were performed for ten distributions of errors and the statistics of the results compiled. Calculations were also made for deviations twice as large as above and the results are given in Fig. 21 together with the error-free case. The feed network reported by Ricardi, et al., [2] displays peak errors of about ± 0.5 dB in power and $\pm 10^\circ$ in phase and therefore approximates the computer model with the smaller random deviations. Such deviations do not lead to appreciable performance degradations. In the null steering mode a different situation exists, however. In this mode two adjacent feeds are excited with signals whose phases are $+90^\circ$ and -90° , respectively, as compared to the phase of the signals applied to the other feeds, and the null is steered by varying the ratio of power fed to the two out-of-phase feeds. The effect of phase errors on the quadrature-fed elements is appreciable as may be inferred from Fig. 22 where the 15-dB contour of the steered null corresponding to a power ratio of 1 (reproduced from Fig. 17) is shown together with those obtained when signals of phase 93° and -93° and also 96° and -96° , are applied. A phase error of 3° causes the 15-dB gain reduction coverage to contract and a phase error of 6° causes a splitting of this coverage. Thus to maintain the coverage the phase error at the feed must not exceed a couple of degrees. Since

EFFECT OF FEED EXCITATION ERRORS

18-6-16808

3σ power (dB)	3σ phase (deg)	ECG _{min} (dB)		ECG _{max} (dB)		Ripple (dB)		Null Depth (dB)	
		Mean	Std Dev	Mean	Std Dev	Mean	Std Dev	Mean	Std Dev
0	0	19.3	-	20.8	-	1.5	-	37.3	-
0.5	15	19.2	0.2	20.8	0.2	1.7	0.3	36.9	3.0
1.0	30	18.0	0.2	21.1	0.3	2.3	0.3	33.9	4.3

Fig. 21. Effect on performance of feed excitation errors.

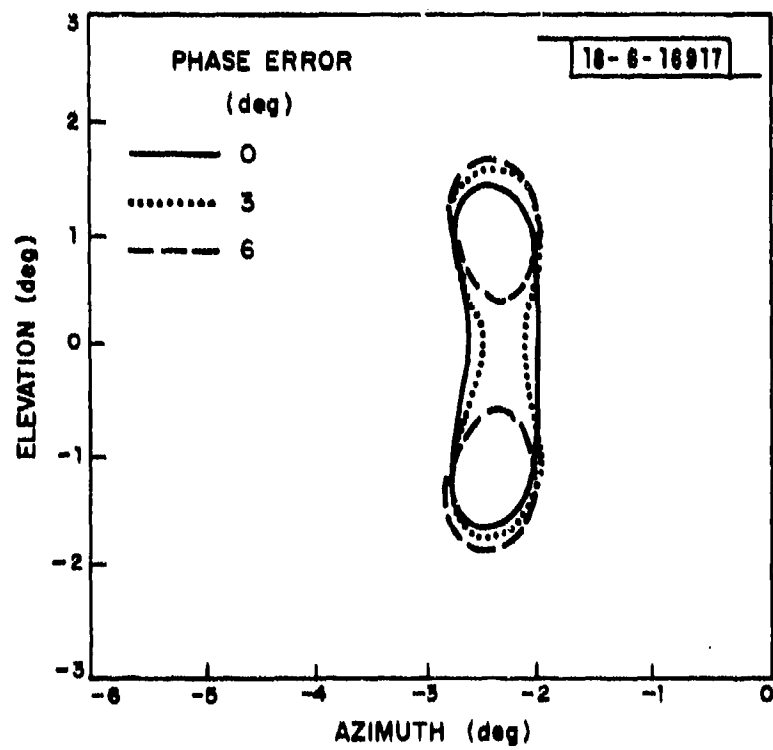


Fig. 22. Effect of phase errors on steered null.

both the beam-forming network and the required 3-state phase shifter contribute to phase errors, a tight tolerance of the order of about $\pm 1^\circ$ is imposed on each of these units, which may be difficult to achieve in practice. In the alternative nulling technique described next, such tight tolerances are not required. This technique involves replacement of the feed cluster by a cluster with a higher density of elements and therefore has the disadvantage of requiring a larger number of variable power dividers in the beam-forming network.

V. Alternative Nulling Technique

Consider the replacement of each feed of the optimally designed 19-feed cluster by three smaller feeds. It would then be expected that suppressing excitation to groups of three adjacent feeds would produce a null about similar to that obtained by suppressing excitation to the larger single feed they replaced. That this is actually the case was verified by computing the performance of a 28-inch lens with a cluster of 61 feeds. Optimization of this configuration led to a feed spacing of 1.3 inches, i.e., $\approx 1/\sqrt{3}$ times the spacing of the optimum 19-feed configuration. The 61-feed cluster is shown in Fig. 23. Since a null is produced by suppressing excitation to groups of three adjacent feeds and since such groups overlap, their null coverages also overlap. Figure 24 shows the 15-dB gain reduction contours obtained by suppressing excitation to each group of three adjacent feeds contained in a 7-feed sub-cluster, demonstrating that in all directions within a corresponding cell of coverage a gain reduction of at least 15 dB is achieved. Since the full FOV is generated by translations of this cell of coverage and since these cells may be made to overlap it follows that this gain reduction applies to the full FOV.

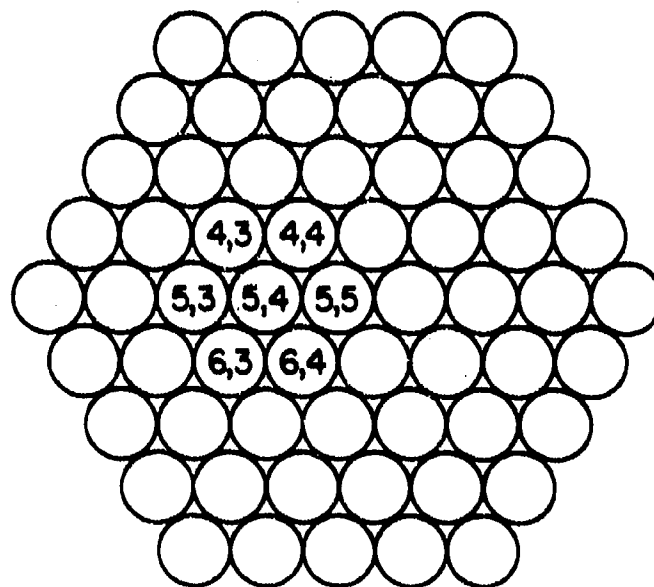


Fig. 23. Feed geometry.

WAVEGUIDE LENS AND 61-ELEMENT FEED CLUSTER
LENS DIAM = 28 in. FEED SPACING = 1.30 in. F/D = 1
DESIGN FREQUENCY = 8.15 GHz FREQUENCY = 8.15 GHz
UNIT FEEDS PHASE CORRECTED CIRCULAR POLARIZATION
GROUPS OF 3 FEEDS OFF

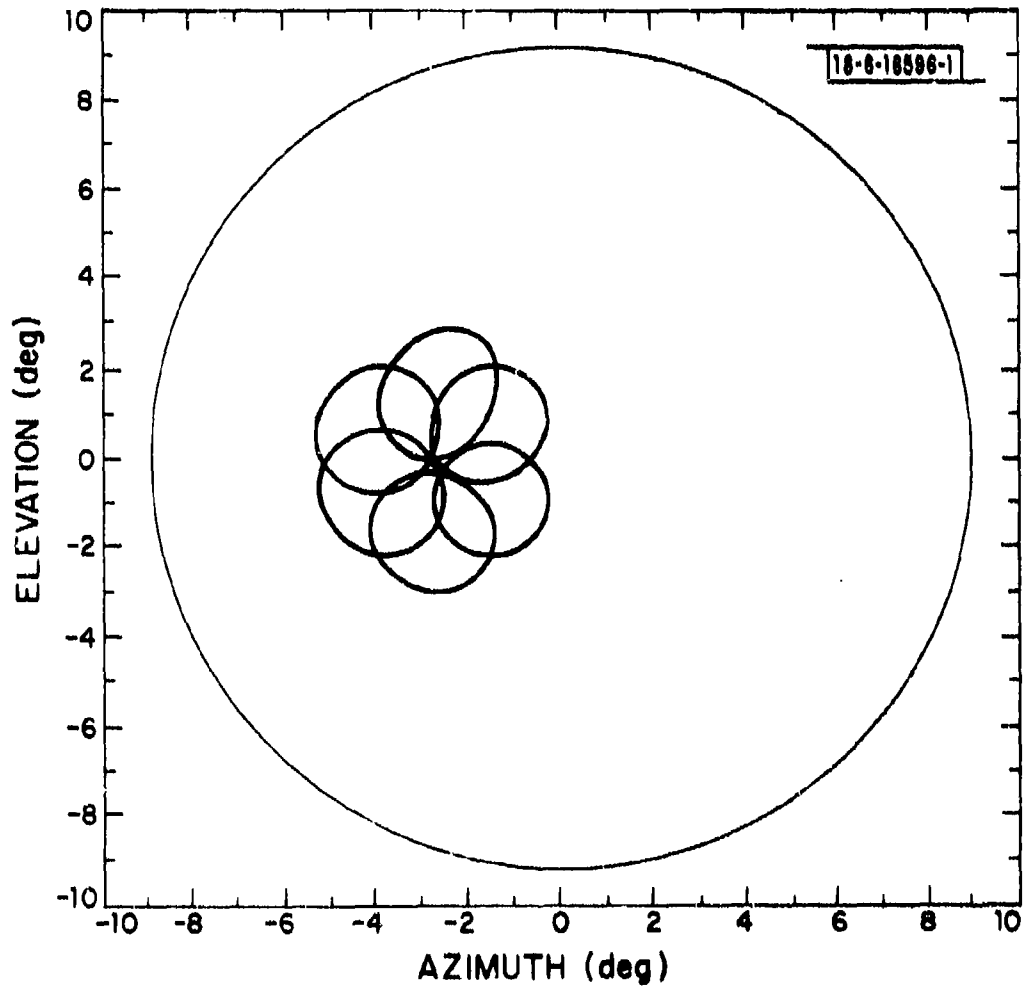


Fig. 24. Coverage of overlapping nulls.

This technique, which could appropriately be called virtual overlapping feed technique, is capable of static gain reductions larger than 15 dB with a simple extension of the process. This capability exists because the phase of the radiation is nearly uniform over most of the angular extent of a null and this phase is also nearly equal to the phase of the radiation over the narrow beam associated with the feeds whose excitations are suppressed. Consequently, by letting a small amount of power leak to these feeds and reversing the polarity of the radiated field the resulting level of radiation in directions within the null may be appreciably reduced. The 15-dB gain reduction contour corresponding to removal of excitation to feeds 43, 54 and 55 (included in the presentation of Fig. 24) is shown enlarged as the heavy line in Fig. 25, while the coverage of 25 dB or more reduction is shown by the dotted area in this Figure. Also shown are the annular areas where the gain is reduced by more than 25 dB when these three feeds are excited 180° out of phase with all other feeds and at a relative power level $P_L = -16.5$ dB and -12.0 dB. Note that the gain is reduced more than 25 dB over the areas shown only when the excitation is as indicated; specifically the gain reduction in the dotted area is less than .25 dB when $P_L = -16.5$ or -12.0 dB. Thus with only three settings of the power level to these feeds the gain can be reduced by more than 25 dB over a coverage identical to the 15-dB or more gain reduction coverage obtained by simply removing excitation to these feeds. Since this latter gain reduction can be accomplished anywhere within the FOV, so can the 25-dB gain reduction. The required values of power setting are not identical for all 7-feed sub-clusters however, and it should be observed that with polarity reversal deep

WAVEGUIDE LENS WITH 61-ELEMENT FEED CLUSTER
 LENS DIAM = 28 in. FEED SPACING = 1.30 in. F/D = 1
 DESIGN FREQUENCY = 8.15 GHz FREQUENCY = 8.15 GHz
 UNIT FEEDS PHASE CORRECTED CIRCULAR POLARIZATION
 FEEDS 4,3 5,3 AND 5,4 DRIVEN OUT OF PHASE AND WITH POWER
 LEVEL P_L WITH RESPECT TO ALL OTHER FEEDS

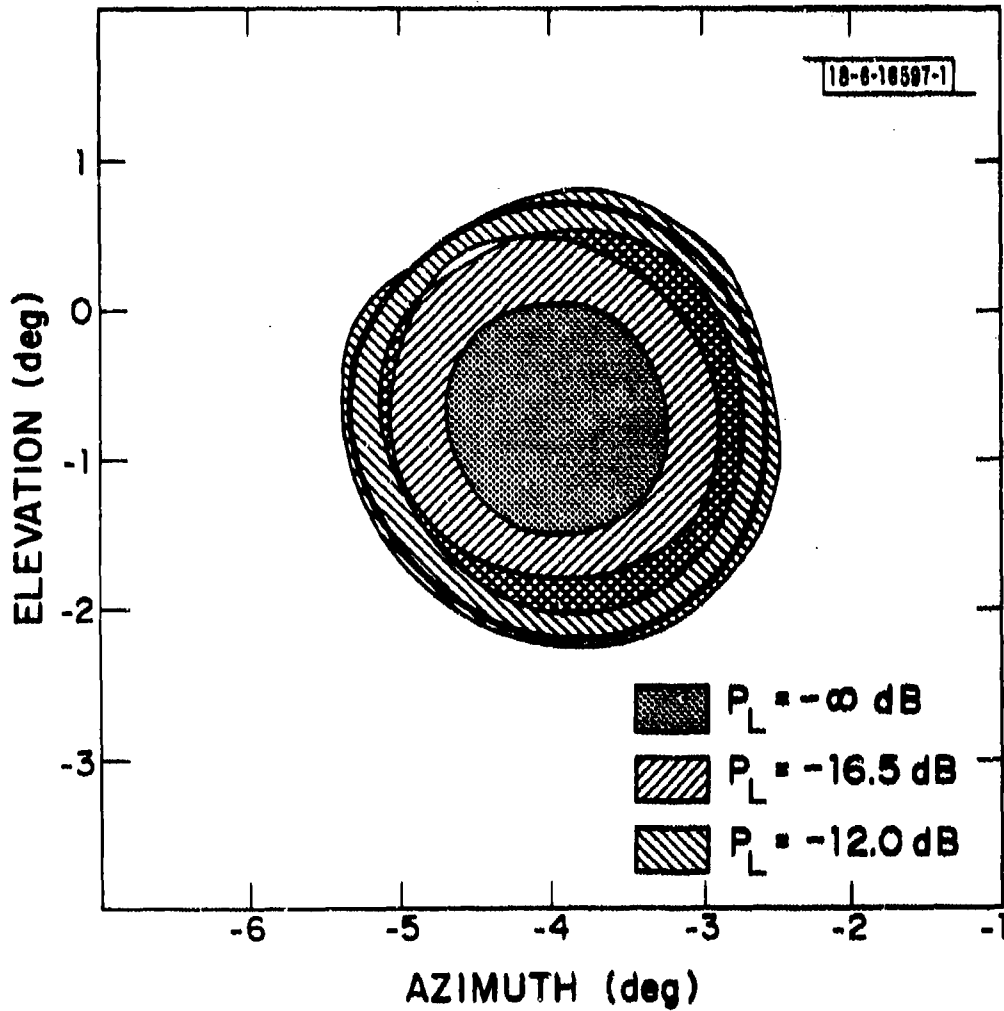


Fig. 25. Coverages of 25-dB or more gain reduction.

nulling can also be accomplished by adjusting the power level to but one feed. The desirable characteristics of the virtual feed overlapping technique remain to be confirmed over a finite bandwidth and for feed excitation errors of practical magnitudes. Since only a reversal of polarity is required, a close control of phase is not necessary and there seems to be no reason why the performance of the 61-beam MBA would degrade more with feed excitation errors than that of the reported 19-beam MBA. Reversal of polarity is an inherent characteristic of the variable power divider considered by Ricardi, et al. [2] but its size and weight could preclude its use in an implementation of the technique.

VI. Discussion

The optimum dimensions of a multiple-beam antenna for communication-satellite applications were derived for two separate systems 1) a transmit area-coverage system realized by narrow-beam switching and 2) a receive earth-coverage beam system with nulls in specified directions. The optimum dimensions of these two systems are very closely identical and therefore, in principle the two systems could be implemented with a single lens and feed cluster.

The nulling earth-coverage antenna with a 19-feed cluster requires a tight phase tolerance on feed excitations except in applications where the large nulling areas associated with suppressed excitations to 2 or 3 adjacent feeds are tolerable. A virtual feed overlapping technique relieves the system from such tight tolerances as demonstrated by the performance of a 28-inch diameter lens with a 61-feed cluster. The much larger feed network of this system could be objectionable, however. Of related interest is the performance of a 37-feed cluster that was briefly studied but not reported above. Its optimum performance is reached with a lens diameter of 24 inches and a

feed spacing of 1.35 inch. With excitations to three adjacent feeds suppressed, a performance similar to that of the 61-feed configuration is obtained but with a 15-dB null width about 1.3 times larger. Indications are that the 37-feed configuration is appreciably more frequency sensitive than the 61-feed configuration but the much reduced size of its feed network nevertheless makes further characterization of its performance desirable.

APPENDIX A

Derivation of the Directive Gain Functions

Consider the feed cluster and lens geometry of Fig. 26 and let P be the power at the input of the $1:N_F$ power divider where N_F is the number of feeds in the cluster. The power radiated by feed i,j is P/N_F of which the amount P_A absorbed by the lens waveguide element m,n is given by

$$P_A = (P/N_F) (G_o f_{mnij}^2 / 4\pi r_{mnij}^2) (a^2 \cos^2 \beta_{mnij} / \cos \alpha_{mn}) (1 - \Gamma_{mn}^2)$$

where

$G_o f_{mnij}^2$ is the gain of feed i,j in the direction of waveguide m,n (see Note 1)

G_o is the feed directivity

r_{mnij} is the distance between the feed and the waveguide element

$a^2 \cos^2 \beta_{mnij} / \cos \alpha_{mn}$ is the absorbing cross section of the waveguide element

and

Γ_{mn} is the reflection coefficient at the input of a waveguide element and is given by

$$\Gamma_{mn} = \frac{2(\nu-1)}{\nu+1} \sin \left(\frac{2\pi \nu d_{mn}}{\lambda} \right)$$

where

d_{mn} is the length of the waveguide element and

where

$$F(\theta, \phi) = \sum_m \sum_n \sum_i \sum_j \frac{h(\theta, \phi) f_{mni} \cos^{1/2} \beta_{mni}}{\left(\frac{r_{mni}}{f}\right) \cos^{1/2} \alpha_{mn}} \exp[-jk(r_{mni} + v d_{mn} - \vec{p}_{mn} \cdot \vec{\mu})]$$

and f is the focal length of the lens.

The power density is

$$F(\theta, \phi) = \frac{|E(\theta, \phi)|^2}{2 \left(\frac{\mu}{\epsilon}\right)^{1/2}} = \frac{P G_o a^4}{4\pi N_F R^2 \lambda^2 f^2} |F(\theta, \phi)|^2$$

and since $P/4\pi R^2$ is the isotropic level of radiation the directive gain function is

$$G(\theta, \phi) = \frac{G_o a^4}{N_F f^2 \lambda^2} |F(\theta, \phi)|^2$$

Note 1: The foedhorn radiation function f is of the form

$$f = (1 - u^2/6 + u^4/120) (1 - v^2/6 + v^4/120)$$

with

$$u = \frac{\pi d_E}{\lambda} \cos \beta_x$$

$$v = \frac{\pi d_H}{\lambda} \cos \beta_y$$

where $\cos \beta_x$ and $\cos \beta_y$ are direction cosines of r_{mni} . The parameters d_E and d_H were obtained by fitting f to the measured E- and H-plane radiation patterns of a 2-inch aperture conical horn excited with a TE_{11} mode.

$$v = [1 - (\lambda/2a)^2]^{1/2}$$

is the index of refraction of the lens.

The power absorbed at one end of each waveguide element propagates unattenuated to the other end where it is radiated. At a far-field distance R and in near-axial direction θ, ϕ the electric field generated is given by

$$h(\theta, \phi) \left[P_A \left(\frac{2(\frac{\mu}{\epsilon})^{1/2}}{4\pi R^2} \right) \left(\frac{4\pi a^2}{\lambda^2} \right) \right]^{1/2} \exp[\cdot jk(r_{mnij} + v d_{mn} - \vec{\rho}_{mn} \cdot \vec{\mu})]$$

where

$(\frac{\mu}{\epsilon})^{1/2}$ is the characteristic impedance of free space

$k = \frac{2\pi}{\lambda}$ λ is the wavelength of the radiation

$\frac{4\pi a^2}{\lambda^2}$ is the aperture gain of the waveguide element

$h(\theta, \phi)$ is the amplitude radiation pattern of a waveguide element (see Note 2)

$\vec{\rho}_{mn}$ is the vector position of element m, n at the exit side

$\vec{\mu} = \sin\theta\cos\phi\vec{i}_x + \sin\theta\sin\phi\vec{i}_y + \cos\theta\vec{i}_z$ is the unit direction vector.

The vector $\vec{\rho}_{mn}$ and $\vec{\mu}$ are referred to a rectangular coordinate system parallel to the coordinate system of Fig. 26 and with origin at O_2

The field radiated by the antenna is obtained by summing the contribution from each waveguide element and each feedhorn or

$$E(\theta, \phi) = \left[\frac{2(\frac{\mu}{\epsilon})^{1/2} P_G a^4}{4\pi N_F R^2 \lambda^2 F^2} \right]^{1/2} F(\theta, \phi)$$

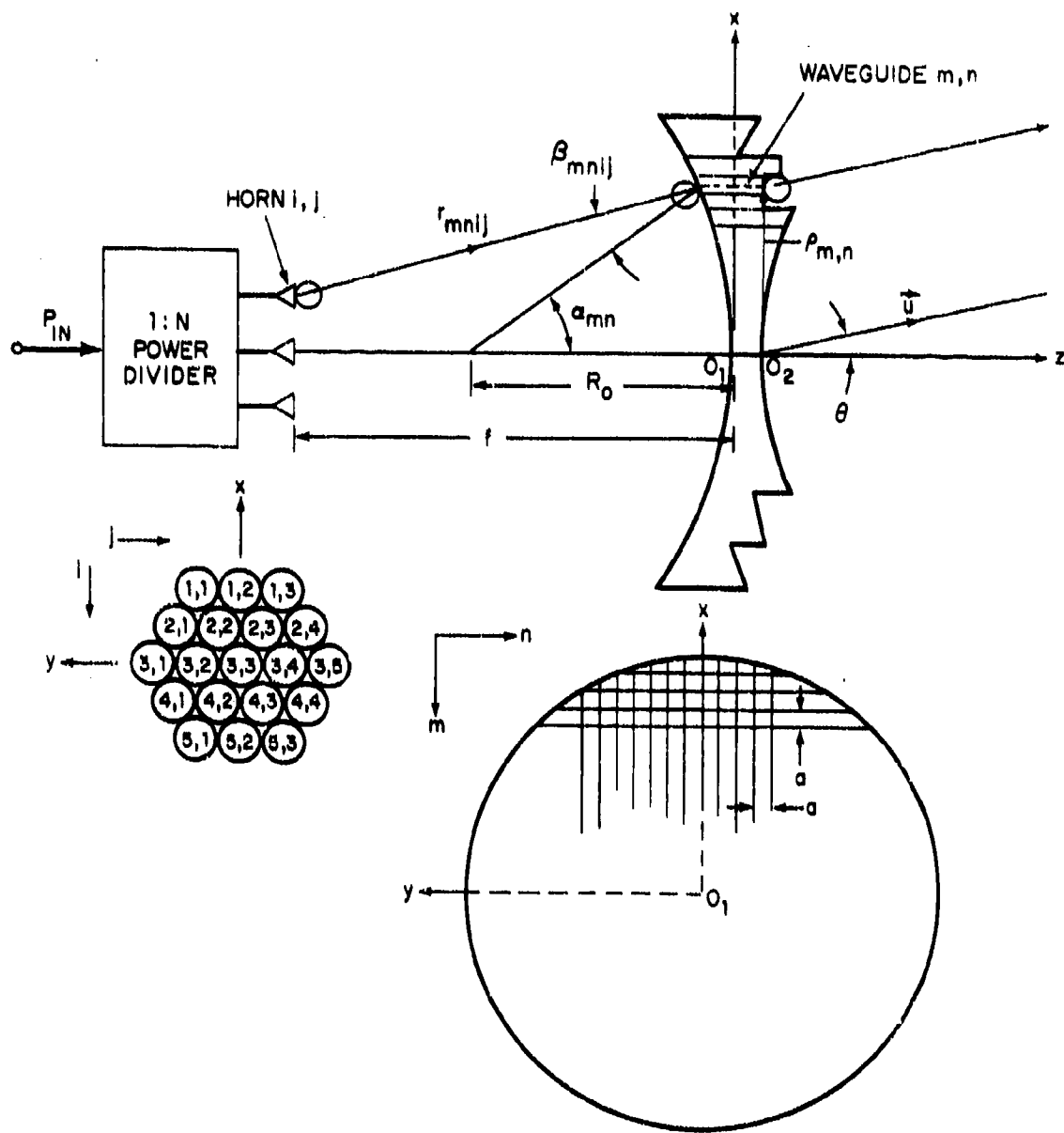


Fig. 26. Waveguide lens and feed cluster geometry.

The gain $G_0 = (\pi d_{\text{EFF}}/\lambda)^2$ where d_{EFF} , the effective diameter of the feed-horns, is deduced from the measured gain of the 2-inch horn.

Note 2 : The amplitude radiation pattern of the waveguide elements is unity except for elements adjacent to a step where it is made equal to the radiation pattern of a waveguide element adjacent to an infinite ground plane.

With the electric vector parallel to the ground plane

$$h_H(\theta, \phi) = 2\sin^2 U + 2j\sin U \cos U$$

and with the electric vector perpendicular to the ground plane

$$h_E(\theta, \phi) = 2\cos^2 V - 2j\cos V \sin V$$

$h(\theta, \phi) = 0$ for direction below the ground plane

$$U = \frac{\pi a}{\lambda} \sin \theta \sin \phi$$

$$V = \frac{\pi a}{\lambda} \sin \theta \cos \phi$$

Computation of Lens Geometry

The lens geometry is derived under the condition that a wave issued from a point source at the focal point is transformed by the lens into a plane wave travelling in the axial direction. This condition is met with

$$d_{mn} - d_0 = \frac{[(f + Z_1(m, n))^2 + x^2 + y^2]^{1/2} - f - Z_1(m, n)}{1 - v}$$

where $Z_1(m, n) = (R_0^2 - x^2 - y^2)^{1/2} - R_0$

R_0 is the radius of the inner spherical surface of the lens

d_0 is the thickness of the lens on axis

x and y are, respectively, the abscissa and ordinate of waveguide element m, n

The length of a waveguide element is reduced by $\frac{\lambda_0}{1-v_0}$ whenever

$$d_{mn} - d_0 \geq \frac{\lambda_0}{1-v_0}$$

where $v_0 = [1 - (\lambda_0/2a)^2]$ and λ_0 is the lens design wavelength.

Computer Program

The FORTRAN IV computer program listed below requires the following input data:

Input Data

List 1 -- Lens Geometry

- WL: design wavelength of lens
- D: lens diameter
- A: width of the waveguide elements of the lens
- TAU: thickness of wall of the waveguide elements of the lens
- DZRO: thickness of lens on axis
- FOD: F/D ratio
- RADIN: radius of the inner surface of the lens.
- LENSPR: printout indicator for lens geometry (set LENSPR = 1 for printout)
- IPLOT: plot indicator for lens geometry (set IPLOT = 1 for SC4060 plots)
- NPLOT: incremented index to identify various runs

List 2 -- Feed Geometry

- WLO: wavelength
- SPACE: spacing between feeds
- IFEED: number of rows in feed cluster, e.g., IFEED = 5 for 19-element feed cluster.

JFEED(I): number of feeds in each row, i.e., JFEED(1) = 3, 4, 5, 4, 3
for 19-element feed cluster.

FACLAT: lattice factor = ratio of spacing between rows to spacing
between feeds in a row; FACLAT = 0.866 for triangular
lattice

ION(I): First indices of feeds which are excited

JON(I): Second indices of feeds which are excited, e.g.,
ION(1) = 3, 18*0, JON(1) = 3, 18*0 means feed 3, 3 is
excited

ION(1) = 3, 2, 1, 16*0

JON(1) = 2, 1, 2, 16*0

means feeds 3, 2, 2, 1 and 1, 2 are excited

NFDON: number of feeds excited

NOTE: IFEED and JFEED(I) cannot be made larger than 5 without redimen-
sioning the array variables ION and JON

IPOL: IPOL = 1 linear polarization with E-vector along X-axis
IPOL = 2 circular polarization

List 4 -- Field Geometry

PHI: angle of pattern cut
PHI = 0 E-plane cut
PHI = 90 H-plane cut

TFIRST: initial θ from axis

TLAST: last θ from axis

DELT: increment of θ for which field is calculated

ICARD: Option card for next set of data
ICARD = 2 Go to Read List 4
ICARD = 1 Go To Read List 2
ICARD \neq 1 or 2 Go To Read List 1

All lengths are in inches, angles in degrees

Output

The output data consist of

1. input data
2. Z-coordinates of waveguide lens vs m,n
3. directivity
4. relative gain vs angle off axis for a given plane of cut
5. SC 4060 plots

It should be noted that much of the data reported in this document required some slight modifications to the computer program which are not included in the following listing. For instance the unit feed, the phase correction and the variable feed excitation coefficients are not dealt with.

```

*****COMPUTER PROGRAM*****
DIMENSION Z1(50,50),Z2(50,50),NCON(50),NFIN(50),RDSQ(50,50).
1 PWR(100),T(100),NGUIDE(50),FHZ(100)
DIMENSION JFEED(10),NPSX(10),NPSY(10,10),NPSQ(10,10)
DIMENSION ION(25),JON(25)
DIMENSION ISTEP(50,50)
DIMENSION ZCOR(2),PATH2(2)
COMPLEX FEEDF
COMPLEX FIELD,FIELDE,FIELDH,FIELDF(50,50,2)
COMPLEX ANPH(2),ANPN(2)
NAMELIST/LIST1/WL,D,A,TAU,DZRO,FOD,RADIN,LENLSPR,IPL0T,NPLOT
1 /LIST2/WLO,SPACE,IFEED,JFEED,FACLAT,ION,
2JON,NFDON,IPOI
3/LIST4/PHI,TFIRST,TLAST,DELTA,ICARD
FUNC(X,Y,RADIN)=SQRT(RADIN**2-X**2-Y**2)-RADIN
CRAD=0.17453293E-1
TWOPI=6.2831853
REPO0010
REPO0020
REPO0030
REPO0040
REPO0050
REPO0060
REPO0070
REPO0080
REPO0090
REPO0100
REPO0110
REPO0120
REPO0130
REPO0140
REPO0150
REPO0160
REPO0170
REPO0180
REPO0190
REPO0200
REPO0210
REPO0220
REPO0230
REPO0240
REPO0250
REPO0260
REPO0270
REPO0280
REPO0290
REPO0300
REPO0310
REPO0320
REPO0330
REPO0340
REPO0350
REPO0360
REPO0370
REPO0380
REPO0390
REPO0400
REPO0410
REPO0420
REPO0430
REPO0440
REPO0450
REPO0460
REPO0470
REPO0480
REPO0490
REPO0500
REPO0510
REPO0520
REPO0530
REPO0540
REPO0550

C
C
C
BEGIN COMPUTATION OF LENS GEOMETRY

150 READ(5,LIST1,END=900)
IF(IPL0T.EQ.1)CALL MODMSG
IF(IPL0T.EQ.1)CALL SCOUTG(98,140,'S')
WRITE(6,2)WL,FOD,D,RADIN,A,TAU,DZRO
2 FORMAT(1H1 2X'WAVELENGTH=' ,F5.3,' IN.' ,/3X'F/D=' ,F5.3,/3X
1'DIAMETER=' ,F5.2,' IN.' ,/3X'RADIUS OF LENS INSIDE SURFACE=' ,F5.2,
1 IN.' ,/3X'WAVEQUIDE I.D.' ,F5.3,' IN.' ,/3X
2'WALL THICKNESS=' ,F6.3,' IN.' ,/3X'LENS THICKNESS ON AXIS=' ,F6.2,
4' IN.' )
DO 313 N=1,50
DO 313 M=1,50
Z1(M,N)=0.0
313 Z2(M,N)=0.0
APT=A+TAU
FL=FOD*D
RINDEX=SQRT(1.-(WL/2./A)**2)
DWAWE=WL/(1.-RINDEX)
WRITE(6,3)RINDEX,DWAWE,FL
3 FORMAT(3X'INDEX OF REFRACTION=' ,F6.4,/3X'FULL-WAVE STRP=' ,F7.4,
1' IN.' ,/3X'FOCAL LENGTH=' ,F6.2,' IN.' )
HMAX=D/2./APT+.5
NFIN=2.*HMAX
DO 600 M=1,HMAX
NGUIDE(M)=M
X=(-M+HMAX+.5)*APT
NCON(M)=HMAX+1.5-SQRT(2.*(M-.5)*HMAX-(M-.5)**2)
NFIN(M)=2*HMAX-NCON(M)+1
DO 601 N=1,HMAX
IF(N.LT.NCON(M)) GO TO 603
Y=(-M+HMAX+.5)*APT
Z1(M,N)=FUNC(X,Y,RADIN)
DNDZ=SQRT((FL+Z1(M,N))**2+X**2+Y**2)-FL-Z1(M,N)
DNDZ=DNDZ/(1.-RINDEX)
688 IF(DNDZ.GT.DWAWE) GO TO 1000
GO TO 1001

```

1000	DMDZ=DMDZ-DWAVE	REP00560
	GO TO 888	REP00570
1001	Z2(M,N)=Z1(M,N)+DMDZ+DZERO	REP00580
	GO TO 601	REP00590
603	Z1(M,N)=0.	REP00600
	Z2(M,N)=0.	REP00610
601	CONTINUE	REP00620
600	CONTINUE	REP00630
	MMAX1=MMAX+1	REP00640
	DO 750 M=1,MMAX	REP00650
750	Z2(M,MMAX1)=Z2(M,MMAX)	REP00660
	DO 751 M=1,MMAX1	REP00670
751	Z2(MMAX1,N)=Z2(MMAX,N)	REP00680
C		REP00690
C	ISTEP=1 IDENTIFIES STEP ALONG X-AXIS	REP00700
C	ISTEP=2 IDENTIFIES STEP ALONG Y-AXIS	REP00710
C	ISTEP=3 IDENTIFIES STEP ALONG BOTH AXIS	REP00720
C	ISTEP=0 NO STEP	REP00730
		REP00740
	DO 400 M=1,MMAX	REP00750
	NA=NCON(M)	REP00760
	DO 400 N=NA,MMAX	REP00770
	ISTEP(M,N)=0	REP00780
	IF(M.NE.1) GO TO 404	REP00790
	IF(Z2(M,N).LT.Z2(M+1,N)) ISTEP(M,N)=1	REP00800
	GO TO 403	REP00810
404	IF(N.LT.NCON(M-1)) GO TO 402	REP00820
	IF(Z2(M,N).LT.Z2(M-1,N).AND.Z2(M,N).LT.Z2(M+1,N)) ISTEP(M,N)=1	REP00830
403	IF(N.EQ.NA) GO TO 401	REP00840
402	IF(M.EQ.1) GO TO 405	REP00850
	IF(N.LT.NCON(M-1).AND.Z2(M,N).LT.Z2(M+1,N)) ISTEP(M,N)=1	REP00860
405	IF(Z2(M,N).LT.Z2(M,N-1).AND.Z2(M,N).LT.Z2(M,N+1)) ISTEP(M,N)=ISTEP(M,N)+2	REP00870
	GO TO 400	REP00880
401	IF(Z2(M,N).LT.Z2(M,N+1)) ISTEP(M,N)=ISTEP(M,N)+2	REP00890
400	CONTINUE	REP00900
626	DO 630 M=1,MMAX	REP00910
	MMAX1=MMAX+1	REP00920
	DO 630 N=MMAX1,MFIN	REP00930
	MN=MFIN+1-N	REP00940
	ISTEP(M,N)=ISTEP(M,MN)	REP00950
	Z1(M,N)=Z1(M,MN)	REP00960
630	Z2(M,N)=Z2(M,MN)	REP00970
	DO 631 M=MMAX1,MFIN	REP00980
	MM=MFIN+1-M	REP00990
	MGUIDE(M)=M	REP01000
	NCON(M)=NCON(MM)	REP01010
	MFIN(M)=MFIN(MM)	REP01020
	DO 631 N=1,MFIN	REP01030
	ISTEP(M,N)=ISTEP(MM,N)	REP01040
	Z1(M,N)=Z1(MM,N)	REP01050
631	Z2(M,N)=Z2(MM,N)	REP01060
	IF(LENSPR.NE.1) GO TO 702	REP01070
625	NF=1	REP01080
	NL=18	REP01090
		REP01100

104	CONTINUE	REPO1660
C		REPO1670
C	COMPUTE FEED GEOMETRY	REPO1680
C		REPO1690
	DO 250 I=1,IFEED	REPO1700
	MFEEED=JFEED(I)	REPO1710
	EPSX(I)=(-I+IFEED/2.+5)*SPACE*FACLAT	REPO1720
	EPSXSQ=EPSX(I)**2	REPO1730
	DO 250 J=1,MFEED	REPO1740
	EPSY(I,J)=(-J+MFEED/2.+5)*SPACE	REPO1750
250	EPSSQ(I,J)=EPSY(I,J)**2+EPSXSQ	REPO1760
C		REPO1770
C	END OF COMPUTATION OF FEED GEOMETRY	REPO1780
C		REPO1790
	FLSQ=FL**2	REPO1800
	RINDEX=SQRT(1.-(WLO/2./A)**2)	REPO1810
	RHO=(RINDEX-1.)/(RINDEX+1.)	REPO1820
	RHO2=2.*RHO	REPO1830
	WRITE(6,16)(ION(I),JON(I),I=1,19)	REPO1840
16	FORMAT(2X'THE FOLLOWING FEEDS ARE ON',10('(',I2,',',I2,')')/29X	REPO1850
	19('(',I2,',',I2,')'))	REPO1860
	GFEEEA=GFEEED-10.*ALOG10(FLOAT(MFEED))	REPO1870
118	DO 113 M=1,MFIN	REPO1880
	DO 113 M=1,MFIN	REPO1890
	FIELDP(M,M,1)=(0.,0.)	REPO1900
113	FIELDP(M,M,2)=(0.,0.)	REPO1910
	DWH=TWOPI*HORNH/WLO/2.	REPO1920
	DWH=TWOPI*HORNH/WLO/2.	REPO1930
	DO 999 I=1,IFEED	REPO1940
	MFEEED=JFEED(I)	REPO1950
	DO 999 J=1,MFEED	REPO1960
710	FEEDFD=CHPLX(1.,0.)	REPO1970
	MCOUNT=0	REPO1980
	DO 712 IOF=1,IFEED	REPO1990
	MFEEED=JFEED(IOF)	REPO2000
	DO 712 JOF=1,MFEED	REPO2010
	MCOUNT=MCOUNT+1	REPO2020
	IF(I.EQ.ION(MCOUNT).AND.J.EQ.JON(MCOUNT)) GO TO 711	REPO2030
712	CONTINUE	REPO2040
	GO TO 999	REPO2050
711	MFIRST=1	REPO2060
	MLAST=MFIN	REPO2070
	DO 111 M=MFIRST,MLAST	REPO2080
	NA=MCON(M)	REPO2090
	NB=MFIN(M)	REPO2100
	X=(MNAI+.5-M)*APT	REPO2110
	XX=2.*EPSX(I)*X-EPSSQ(I,J)-FL**2	REPO2120
	DO 1113 M=NA,NB	REPO2130
	Y=(MNAI+.5-M)*APT	REPO2140
	PATH1=-XX-2.*EPSY(I,J)*Y+2.*(FL-RADIN)*Z1(M,M)	REPO2150
	PATSQR=SQRT(PATH1)	REPO2160
	SCPR=(X-EPSX(I))/PATSQR	REPO2170
	SSPR=(Y-EPSY(I,J))/PATSQR	REPO2180
	U1=DWH*SCPR	REPO2190
	U2=DWH*SSPR	REPO2200

	U1SQ=U1**2	REP02210
	U2SQ=U2**2	REP02220
	AMPLI=(1.-U1SQ/6.+U1SQ**2/120.)*(1.-U2SQ/6.+U2SQ**2/120.)	REP02230
	AMPLI=AMPLI/SQRT(1.+B1(N,N)/PL)	REP02240
	RRRR=(PL-RADIN)*B1(N,N)+PL*RADIN-SPRX(I)*X-SPSY(I,J)*Y	REP02250
	RRRR=SQRT(RRRR/RADIN/PATSQR)	REP02260
	AMPLI=AMPLI*RRRR	REP02270
	AMPLI=AMPLI*PL/PATSQR	REP02280
	PATH1=PATSQR	REP02290
	PATH1=PATH1*TWOPI/WLO	REP02300
	FIELDP(N,N,1)=FIELDP(N,N,1)+CNPLX(AMPLI,0.)*CNXP(CNPLX(0.,PATH1))	REP02310
	1*FEEDFD	REP02320
	IF(IPOL.NE.2)GO TO 1113	REP02330
	U1=DWR*SSPR	REP02340
	U2=DWR*SCPR	REP02350
	U1SQ=U1**2	REP02360
	U2SQ=U2**2	REP02370
	AMPLI=(1.-U1SQ/6.+U1SQ**2/120.)*(1.-U2SQ/6.+U2SQ**2/120.)	REP02380
	AMPLI=AMPLI*RRRR*PL/PATSQR/SQRT(1.+B1(N,N)/PL)	REP02390
	FIELDP(N,N,2)=FIELDP(N,N,2)+CNPLX(AMPLI,0.)*CNXP(CNPLX(0.,PATH1))	REP02400
	1*FEEDFD	REP02410
1113	CONTINUE	REP02420
111	CONTINUE	REP02430
999	CONTINUE	REP02440
		REP02450
	END OF COMPUTATION OF FIELD AT EXIT OF WAVEGUIDES	REP02460
		REP02470
	BEGIN COMPUTATION OF FAR FIELD	REP02480
		REP02490
18	READ(5,LIST4,END=900)	REP02500
	WRITE(6,17)PHI	REP02510
17	FORMAT(/3X'PHI=',F7.2,'DEGREES')	REP02520
	PHIR=PHI*CRAD	REP02530
	COSPHI=COS(PHIR)	REP02540
	SINPHI=SIN(PHIR)	REP02550
	PWNOR=-100.	REP02560
	THETA=TFIRST	REP02570
	IEND=(TLAST-TFIRST)/DELT+1.5	REP02580
116	DO 110 K=1,IEND	REP02590
	THETAR=THETA*CRAD	REP02600
	SINT=SIN(THETAR)	REP02610
	COST=COS(THETAR)	REP02620
		REP02630
	BEGIN COMPUTATION OF RADIATION PATTERN OF WAVEGUIDE ELEMENTS	REP02640
		REP02650
	SINCOS=SINT*COSPHI	REP02660
	SINSIN=SINT*SINPHI	REP02670
	PIDOL=APT*TWOPI/2./WLO	REP02680
	HPIDOL=ABS(PIDOL*SINCOS)	REP02690
	EPIDOL=ABS(PIDOL*SINSIN)	REP02700
	SINN=SIN(HPIDOL)	REP02710
	SINH=SIN(EPIDOL)	REP02720
	COSN=COS(HPIDOL)	REP02730
	COSH=COS(EPIDOL)	REP02740
	FIELDP=(0.,0.)	REP02750

```

FIELDH=(0.,0.)
NFIRST=1
NLAST=NFIN
DO 112 N=NFIRST,NLAST
NA=NCON(N)
NB=NFIN(N)
DO 1123 M=NA,NB
AMPN(1)=CHPLX(1.,0.)
AMPN(2)=CHPLX(1.,0.)
AMPN(1)=CHPLX(1.,0.)
AMPN(2)=CHPLX(1.,0.)
ZCOR(1)=Z2(N,M)
ZCOR(2)=Z2(N,M)
IF(ISTEP(N,M).GE.2) GO TO 410
GO TO 411
410 IF(SINT*SINPHI.GE.0..AND.N.LE.NMAX) GO TO 420
IF(SINT*SINPHI.LE.0..AND.N.GT.NMAX) GO TO 420
AMPN(1)=CHPLX(0.,0.)
AMPN(2)=CHPLX(0.,0.)
GO TO 1123
420 AMPN(1)=CHPLX(2.*SINH*SINH,+2.*SINH*COSH)
IF(N.EQ.NA.OR.N.EQ.NB)GO TO 431
ZCOR(1)=AHIN1(Z2(N,M-1),Z2(N,M+1))
431 IF(IPOL.NE.2) GO TO 430
ACOF=2.
IF(SINSIN.EQ.0.) ACOF=1.
AMPN(2)=CHPLX(ACOF*COSH*COSH,-ACOF*COSH*SINH)
430 IF(ISTEP(N,M).EQ.2) GO TO 120
411 IF(ISTEP(N,M).EQ.0) GO TO 120
IF(SINT*COSPFI.GE.0..AND.N.LE.NMAX) GO TO 421
IF(SINT*COSPFI.LE.0..AND.N.GT.NMAX) GO TO 421
AMPN(1)=CHPLX(0.,0.)
AMPN(2)=CHPLX(0.,0.)
GO TO 1123
421 ACOF=2.
IF(SINT*COSPFI.EQ.0.) ACOF=1.
AMPN(1)=CHPLX(ACOF*COSH*COSH,-ACOF*COSH*SINH)
IF(IPOL.NE.2) GO TO 120
AMPN(2)=CHPLX(2.*SINH*SINH,+2.*SINH*COSH)
IF(N.EQ.1.OR.N.EQ.NFIN) GO TO 120
IF(N.LE.NMAX.AND.(N.LT.NCON(N-1).OR.N.GT.NFIN(N-1)))GO TO 120
IF(N.GT.NMAX.AND.(N.LT.NCON(N+1).OR.N.GT.NFIN(N+1)))GO TO 120
ZCOR(2)=AHIN1(Z2(N-1,M),Z2(N+1,M))
C
C
C
END OF COMPUTATION OF RADIATION PATTERN OF WAVEGUIDE ELEMENTS
120 PATH=APT*((-N+NMAX+.5)*COSPFI+(-N+NMAX+.5)*SINPHI)*SINT
PLEMS=(Z2(N,M)-Z1(N,M))*RINDEX
FIRO=TWOPI*PLEMS/WLO
ROIN=RHO2*SIN(FIRO)
AMREFP=SQRT(1.-ROIN**2)
PATH2(1)=(ZCOR(1)-Z1(N,M))*RINDEX-PATH-(ZCOR(1)-DERO)*COST
PATH2(2)=(ZCOR(2)-Z1(N,M))*RINDEX-PATH-(ZCOR(2)-DERO)*COST
PATH2(1)=PATH2(1)*TWOPI/WLO
PATH2(2)=PATH2(2)*TWOPI/WLO

```

RNP02760
 RNP02770
 RNP02780
 RNP02790
 RNP02800
 RNP02810
 RNP02820
 RNP02830
 RNP02840
 RNP02850
 RNP02860
 RNP02870
 RNP02880
 RNP02890
 RNP02900
 RNP02910
 RNP02920
 RNP02930
 RNP02940
 RNP02950
 RNP02960
 RNP02970
 RNP02980
 RNP02990
 RNP03000
 RNP03010
 RNP03020
 RNP03030
 RNP03040
 RNP03050
 RNP03060
 RNP03070
 RNP03080
 RNP03090
 RNP03100
 RNP03110
 RNP03120
 RNP03130
 RNP03140
 RNP03150
 RNP03160
 RNP03170
 RNP03180
 RNP03190
 RNP03200
 RNP03210
 RNP03220
 RNP03230
 RNP03240
 RNP03250
 RNP03260
 RNP03270
 RNP03280
 RNP03290
 RNP03300

```

FIELD=FIELD+FIELDP(N,N,1)*CHXP(CMPLX(0.,PATH2(1)))*ANFN(1)      REPO3310
1*ANFN(1)*CHPLX(ANFRF,0.)                                         REPO3320
IF(IPOL.NE.2)GO TO 1123                                           REPO3330
FIELDN=FIELD+FIELDP(N,N,2)*CHXP(CMPLX(0.,PATH2(2)))*ANFN(2)    REPO3340
1*ANFN(2)*CHPLX(ANFRF,0.)                                         REPO3350
1123 CONTINUE                                                    REPO3360
112 CONTINUE                                                       REPO3370
FIELD=FIELD                                                       REPO3380
IF(IPOL.EQ.2) FIELD=0.5*(FIELDN+FIELDH)                           REPO3390
FEZ(K)=ATAN2(AIMAG(FIELD),REAL(FIELD))/CRAD                       REPO3400
FABSO=CABS(FIELD)*APT**2                                          REPO3410
PWR(K)=GFEDA+20.*ALOG10(FABSO)                                    REPO3420
IF(PWR(K).GT.PWNOR) GO TO 878                                     REPO3430
GO TO 879                                                         REPO3440
878 PWNOR=PWR(K)                                                  REPO3450
FEZNOR=FEZ(K)                                                     REPO3460
879 T(K)=THETA                                                    REPO3470
110 THETA=THETA+DELT                                             REPO3480
C                                                                    REPO3490
C PRINT AND PLOT STATEMENTS                                       REPO3500
C                                                                    REPO3510
DO 501 K=1,IEND                                                  REPO3520
PWR(K)=PWR(K)-PWNOR                                             REPO3530
501 FEZ(K)=FEZ(K)-FEZNOR                                         REPO3540
WRITE(6,502) PWNOR,FEZNOR                                       REPO3550
502 FORMAT(/7X 'PEAK GAIN=',F7.2,' DB',5X'REFERENCE PHASE=',F7.2,' DEGREE' REPO3560
10X'ES')
WRITE(6,8) (T(I),PWR(I),FEZ(I),I=1,IEND)                         REPO3570
8 FORMAT(/5X                                                    REPO3580
1'THETA',10X'DB',9X'PHASE(DEG)',/(5X F6.2,6X F8.2,6X F8.2))    REPO3590
IF(IPLOT.EQ.1)WRITE(6,71) NPLOT                                  REPO3600
71 FORMAT(/10X'PLOT NO ',I3)                                     REPO3610
WRITE(6,72)                                                       REPO3620
72 FORMAT(1H1)                                                    REPO3630
DO 301 I=1,IEND                                                  REPO3640
301 IF(PWR(I).LT.-40.) PWR(I)=-40.                               REPO3650
PWR(IEND)=-40.                                                  REPO3660
IF(IPLOT.NE.1) GO TO 650                                         REPO3670
CALL GRAPHG(IEND,T,PWR,7,'DEGREES',2,'DB',                      REPO3680
149,'MULTIPLE SHAN ANTENNA, WAVEGUIDE LENS---DION D-413')      REPO3690
CALL LINESG(IEND,T,PWR)                                         REPO3700
XST=400                                                          REPO3710
YST=100                                                          REPO3720
WRITE(98,70) XST,YST,NPLOT                                       REPO3730
70 FORMAT(2A4,'PLOT NO ',I3)                                     REPO3740
NPLOT=NPLOT+1                                                    REPO3750
CALL FRAMG                                                       REPO3760
650 CONTINUE                                                     REPO3770
IF(ICARD.EQ.1) GO TO 151                                         REPO3780
IF(ICARD.EQ.2)GO TO 18                                          REPO3790
GO TO 150                                                         REPO3800
900 IF(IPLOT.EQ.1)CALL EXITG                                     REPO3810
RETURN                                                            REPO3820
END                                                                REPO3830

```

References

1. A. R. Dion and L. J. Ricardi, "A Variable-Coverage Satellite Antenna System," Proc. IEEE 59, 252-262 (1971), DDC AD-728/90.
2. L. J. Ricardi, et al., "Some Characteristics of a Communication Satellite Multiple-Beam Antenna," Technical Note 1975-3, Lincoln Laboratory, M.I.T. (28 January 1975), DDC AD-A006405.

OUTSIDE DISTRIBUTION LIST

Army

Lt. Colonel J. D. Thompson
ATTN: DAMO-TCS
Department of the Army
Washington, D.C. 20310

Mr. D. L. LaBanca
U.S. Army Satellite Communications
Agency
ATTN: AMCPM-SC511
Building 209
Fort Monmouth, N. J. 07703

Headquarters
Department of the Army
ATTN: DAMA-CSC
Washington, D.C. 20310

Navy

Dr. R. Connley
Office of Chief of Naval Operations
ATTN: 094H
Department of the Navy
Washington, D.C. 20350

Captain S. B. Wilson
Office of Chief of Naval Operations
ATTN: 941P2
Department of the Navy
Washington, D.C. 20350

Mr. D. McClure
Office of Naval Telecommunications
System Architect
3801 Nebraska Avenue
Washington, D.C. 20390

LCDR George Burman
Naval Electronics Systems Command
Headquarters
ATTN: PME-106
Department of the Navy
Washington, D.C. 20350

Marine Corps

Major G. P. Criscuolo
ATTN: CE
Headquarters, U.S. Marine Corps
Washington, D.C. 20380

Air Force

Colonel J. C. Mayers
ATTN: RDSC
Headquarters, U. S. Air Force
Washington, D.C. 20330

Lt. Colonel J. C. Wright
ATTN: PRCKP
Headquarters, U.S. Air Force
Washington, D. C. 20330

JCS

Lt. Colonel J. S. Tuck
Organization Joint Chiefs of Staff
ATTN: J-6
Washington, D.C. 20301

Mr. S. L. Stauss
Organization Joint Chiefs of Staff
ATTN: J-3
Washington, D.C. 20301

NSA

Mr. George Jelen, Jr.
National Security Agency
ATTN: S-26
Ft. George G. Meade, Md. 20755

Mr. David Bitzer
National Security Agency
ATTN: R-12
Ft. George G. Meade, Md. 20755

TRI-TAC

Mr. Paul Forrest
TRI-TAC
Ft. Monmouth, N. J. 07703

DCA

Capt. Register or Capt. Lauber
SAMSO
P. O. Box 92960
Worldway Postal Center
Los Angeles, CA 90009
(20 copies)

C. Bredall
Aerospace Corp.
Bldg. 110, R. 1364
2400 El Segundo, Blvd.
El Segundo, CA 90045
(5 copies)

Dr. Frederick E. Bond, Code 800
Defense Communications Agency
8th Street and South Courthouse Road
Arlington, Virginia
(5 copies)

Mr. Troy Ellington
Defense Communications Eng. Center
1860 Wiehle Avenue
R-405
Reston, Virginia 22090
(2 copies)

C. Sletten
Air Force Cambridge Research Lab.
L. G. Hanscom Field
Bedford, MA 01730

